Mechanistic framework to link root growth models with weather and soil physical properties, including example applications to soybean growth in Brazil

De Moraes, Moacir Tuzzin; Bengough, A. Glyn; Debiasi, Henrique; Franchini, Julio Cezar; Levien, Renato; Schnepf, Andrea

Published in:
Plant and Soil

DOI:
10.1007/s11104-018-3656-z

Publication date:
2018

Document Version
Peer reviewed version

Mechanistic framework to link root growth models with weather and soil physical properties, including example applications to soybean growth in Brazil

Moacir Tuzzin de Moraes, A. Glyn Bengough, Henrique Debiasi, Julio Cezar Franchini, Renato Levien, Andrea Schnepf and Daniel Leitner

Keywords crop model; root growth model; soil compaction; soil strength; crop yield

Abstract

Background and aims Root elongation is generally limited by a combination of mechanical impedance and water stress in most arable soils. However, dynamic changes of soil penetration resistance with soil water content are rarely included in models for predicting root growth. Better modelling frameworks are needed to understand root growth interactions between plant genotype, soil management, and climate. Aim of paper is to describe a new model of root elongation in relation to soil physical characteristics like penetration resistance, matric potential, and hypoxia.
Methods A new diagrammatic framework is proposed to illustrate the interaction between root elongation, soil management, and climatic conditions. The new model was written in Matlab®, using the root architecture model RootBox and a model that solves the 1D Richards equations for water flux in soil. *Inputs:* root architectural parameters for Soybean; soil hydraulic properties; root water uptake function in relation to matric flux potential; root elongation rate as a function of soil physical characteristics. *Simulation scenarios:* (a) compact soil layer at 16 to 20 cm; (b) test against a field experiment in Brazil during contrasting drought and normal rainfall seasons.
Results (a) Soil compaction substantially slowed root growth into and below the compact layer. (b) Simulated root length density was very similar to field measurements, which was influenced greatly by drought. The main factor slowing root elongation in the simulations was evaluated using a stress reduction function.
Conclusion The proposed framework offers a way to explore the interaction between soil physical properties, weather and root growth. It may be applied to most root elongation models, and offers the potential to evaluate likely factors limiting root growth in different soils and tillage regimes.

Introduction

Root growth, and root elongation in particular, can be limited by many factors in the soil environment, including plant pathogens, mineral element toxicities or deficiencies (Foy 1992), temperature (Licht and Al-Kaisi 2005), water availability (Bengough et al. 2011) aeration (Valentine et al. 2012), and soil strength (Bengough 1997). In terms of physical limitations to root growth, water stress (too little water for root growth), hypoxia or anoxia (too little or no oxygen), and mechanical impedance (soil that is too hard for roots to penetrate rapidly) are often major causes of poor root system growth and development (Bengough et al. 2011). Various processes and mechanisms are involved in maintaining root elongation under water stress, such as osmotic adjustment and enhanced cell wall loosening (Wu and Cosgrove 2000; Schmidt et al. 2013). Penetrometer resistance in excess of 2 MPa is generally thought to present a substantial limitation to root elongation rates, and has been used as a simple threshold for characterising soil physical quality (Taylor et al. 1966; Silva et al. 1994; Lipiec et al. 2012). Penetration resistances of >2 MPa, may occur even in relatively moist arable soils, and frequently slow down root elongation to less than half of its unimpeded rate if continuous cracks or macropores aren't available as low-resistance pathways (Bengough et al. 2011).

There is a need to develop predictive frameworks for understanding plant genotype, soil management, and climate interactions with root system growth: A major problem in applying laboratory-based understanding of root growth is that soil matric potential in the field changes constantly, and can vary spatially and temporally through the soil profile (Bengough 2006). Soil physical stresses and their degree of limitation to root elongation vary greatly between soil types, soil management regimes, and individual growth seasons – making very difficult to

predict the effects of agronomic practices and climate on root growth, without using modelling tools.

Root water uptake is a major component of the terrestrial hydrological cycle. Macroscopic models can estimate transpiration rates under limiting hydraulic conditions using spatial averages of soil and root properties (de Jong van Lier et al. 2008). Empirical models have been used to estimate the reduction function of water uptake due to the matric potential (Feddes et al. 1978) in many simulation models such as Soil-Water-Atmosphere-Plant (SWAP) (Kroes et al. 2008) and Hydrus (Šimůnek and Hopmans 2009). However, the macroscopic root water uptake function should include the preferential uptake from wetter layers using root characteristics (root length density and root diameter) and soil hydraulic status, specifically, the matric flux potential (de Jong van Lier et al. 2008).

To simulate the root architecture distribution, many models still consider simple empirical models (e.g. assuming an exponential root length distribution over depth, e.g. Jones et al. (1991)), or density based root models (Kalogiros et al. 2016). Simplistic models that consider only rooting depth to determine the root water uptake (Hartmann et al. 2017) are rarely related to meaningful descriptions of the effect of soil properties on the root length density profile though time. Thus, in order to improve the macroscopic root water uptake (de Jong van Lier et al. 2013) in the soil water flux models (Tron et al. 2015), 3D root architectural models should be used to take into account dynamic development of root structure (Leitner et al. 2010a; Schnepf et al. 2017), and its interaction with soil properties.

There are many different root system models (Dunbabin et al. 2013), that can be divided into pure root growth models (Hartmann and Šimůnek 2016), which focus on describing the root system's topology (Pagès et al. 2004), and more holistic models, which include several root-environment interaction processes (Javaux et al. 2008; Leitner et al. 2010a). In summary, the most common and current models include RootTyp (Pagès et al. 2004), SimRoot (Lynch et al. 1997), Rootmap (Diggle 1988b, a), SPACSYS (Wu et al. 2007), R-SWMS (Javaux et al. 2008), Archisimple (Pagès et al. 2014), OpenSimroot (Postma et al. 2017), RootBox (Leitner et al. 2010a, b), and CrootBox (Schnepf et al. 2017) which have been used for a range of root modelling studies (Dunbabin et al. 2013).

The decision to use each root growth model should be related to computer power (Dupuy et al. 2010), availability of input parameters (Bengough 1997) or requirement of the mechanistic understanding of the soil-root interactions (Dunbabin et al. 2013). In most of the root growth models soil strength dynamic effects on root elongation have not been considered.

Mathematical modelling continues to play an important role in our understanding of root growth and plant water uptake (Schnepf et al. 2012), and further improvement of modelling soil processes is necessary to predict effects on ecosystem services such as food production (Vereecken et al. 2016). RootBox is a widely available dynamic 3D root architecture model based on L-Systems[1] (Leitner et al. 2010b) in Matlab® code called RootBox. An advantage of RootBox (Leitner et al. 2010a) over other models is that it is implemented in Matlab in a way that keeps it open for any changes to the model structure (Dunbabin et al. 2013). This model has been used to predict nutrient uptake (Leitner et al. 2010b; Schnepf et al. 2012), growth of arbuscular mycorrhizal fungi (Schnepf et al. 2016), root-hydrology interactions (Tron et al. 2015) and water stress tolerance (Leitner et al. 2014). RootBox has been used to simulate many types of root system, e.g. to simulate 48 root architectures in 16 drought scenarios (Tron et al. 2015) and to model structural attributes for root functional type in 288 simulated root systems (Bodner et al. 2013). Visual comparisons of the root simulation with excavated roots from field conditions are at least qualitatively promising for species including maize, *Anagallis femina*, and *Brassica napus* (Leitner et al. 2010b).

This paper presents a new simple model for root elongation in relation to soil physical characteristics (penetration resistance, water stress, hypoxia or anoxia), and implements the model in RootBox for contrasting soil management regimes. Specifically, it:

- describes the overall model structure and its component sub-models (root architecture; soil water uptake and redistribution including evapotranspiration; root elongation in relation to soil physical properties);
- proposes a new diagrammatic framework to visualise the interactions between root growth, soil management, and weather conditions;
- calibrates the soil strength-water content relation with laboratory data, and then tests it against field experimental data.

[1] Lindenmayer's system for plant architecture modelling (Prusinkiewicz and Lindenmayer 1990).

Simulations are then run relating to

- a hypothetical soil with single compacted layer;
- a test of the model using two years of field data, incorporating a typical rainfall season, and a year of drought.

Material and Methods

The Model: Modelling approach

A model (Fig. 1) was constructed that consisted of (a) the root architecture model RootBox; (b) a soil-water redistribution model using Richards' equation and a water uptake function; (c) a soil-strength function that relates soil strength to soil water status; and (d) a root-stress function to define root elongation rate as limited by soil physical conditions. The components of the model are described in the following sections, together with the input parameters used in a series of simulations scenarios and comparison with field tests.

Root architecture model (RootBox)

Three-dimensional root system architecture was generated using the RootBox model (Leitner et al. 2010a). Root elongation was described as a negative exponential growth function, (Eq. 1), such that in the absence of stress root elongation follows a negative exponential function of time until a predefined maximum root length (k) is reached (Pagès et al. 1989; Leitner et al. 2010b). The maximum root length (k) is calculated for each individual root (Eq. 2) (Leitner et al. 2014) as the sum of the length of basal and apical zones, plus the spacing and number of lateral branches (Fig. 2). Basic rules are applied for simulating root growth, branching, and different types of tropisms, e.g. gravitropism, exotropism, hydrotropism or chemotropism as described by Tron et al. (2015).

The main equation of interest in this work describes the root elongation. Unimpeded root elongation is given by Eq. (1).

$$RL = k\left(1 - exp\left(-\frac{re}{k}t\right)\right) \quad \text{(Eq. 1)}$$

where *RL* is root length (cm), *t* is time (day), *k* the maximum root length (cm) and *re* the initial root elongation (cm day^{-1}).

$$k = l_b + l_a + l_n.(n_b - 1) \quad \text{(Eq. 2)}$$

where *k* is the maximum root length (cm), l_b is the basal zone (cm), l_a is the apical zone (cm), l_n is the inter-spaces between branching (cm), n_b is the maximal number of lateral branches (unit).

New branches emerge only after the distance between root tip and branch has reached the required apical zone length, and they emerge at a user-defined axial branching angle Θ (normal distribution β and random radial angle (drawn from a uniform distribution between $-\pi$ and π).

Soil water redistribution, incorporating root water uptake

Water flux in the soil matrix was modelled in one dimension by solving the Richards' equation (Eq. 3):

$$C(h)\frac{\partial h}{\partial t} = \frac{\partial}{\partial z}\left(K(h)\left(\frac{\partial h}{\partial z} + 1\right)\right) - S(h) \quad \text{(Eq. 3)}$$

where C is the differential water capacity ($\frac{\partial\theta}{\partial h}$) (cm^{-1}), θ is the volumetric soil water content (cm^3 cm^{-3}), h is the soil water pressure head (cm), t is the time (d), K is the unsaturated hydraulic conductivity (cm d^{-1}), z is the depth (cm, positive upward), S is the root water extraction (cm^3 cm^{-3} d^{-1}).

Eq. (3) was solved numerically by a combination of finite difference and finite element methods (Celia and Bouloutas 1990; van Dam and Feddes 2000), as described in van Dam and

Feddes (2000). The relations between θ, h and K (Mualem 1976; van Genuchten 1980) are shown in Eq. 4 and Eq. 5;.

$$\Theta = \frac{\theta-\theta_r}{\theta_s-\theta_r} = (1+|\alpha h|^n)^{\left(\frac{1}{n}\right)-1}, \quad \text{(Eq. 4)}$$

$$K = K_s\Theta^{\lambda}\left(1-\left(1-\Theta^{\frac{n}{(n-1)}}\right)^{1-\left(\frac{1}{n}\right)}\right)^2, \quad \text{(Eq. 5)}$$

in which Θ is the effective saturation; θ is the water content ($cm^3\ cm^{-3}$); θ_s is the saturated water content ($cm^3\ cm^{-3}$); θ_r is the residual water content ($cm^3\ cm^{-3}$) that was estimated by regression for positive values; h is pressure head (cm); K is the hydraulic conductivity unsaturated (cm d^{-1}); Ks is the saturated hydraulic conductivity (cm d^{-1}); and α (cm^{-1}), n and λ are empirical parameters. The value of parameter λ (Eq. 5) was 0.5 (Mualem 1976; van Genuchten 1980).

The initial condition is imposed by specifying the pressure head (h) at depth (z) at time zero (t = 0). The boundary conditions can be of two types, Dirichlet boundary condition, i.e., specification of the pressure head h, or Neumann boundary condition, i.e., specification of a flux *q* through the boundaries (Feddes et al. 1978).

At the lower boundary we assumed that the water table was deep enough to not influence soil water dynamics, setting the gradient of the water pressure head ∂h/∂z is equal to zero (Tron et al. 2015). Thus, the flux was solely driven by gravity and is equal to the unsaturated hydraulic conductivity calculated at this boundary.

At the top soil surface boundary (i.e. soil surface), water flux is solved by the Richards equation (van Dam and Feddes 2000) and depends on crop development (water uptake), meteorological data and soil conditions. The soil can lose water by evaporation or gain water by infiltration. The potential of crop transpiration and soil water evaporation are estimated with the dual crop coefficient (Allen et al. 1998, 2005). For this model, we consider only root growth and neglect shoot development. However, the link between soil-plant-atmosphere is the actual plant transpiration (de Jong van Lier et al. 2008). In case of evaporation, the potential water flux from the soil surface only depends on atmospheric conditions, but the actual flux would be restricted by availability of water in upper soil layers (Tron et al. 2015). If these soil layers dry, the boundary condition will switch from flux-controlled, with *q* equal to the potential evaporation (EP, cm day^{-1}), to head-controlled, with $h = h_{atm}$. The parameter h_{atm} is the water pressure head at the soil surface in equilibrium with the pressure head of the atmosphere (Feddes et al. 1978).

In both cases, as described in Tron et al. (2015) the condition in the Eq. (6) must be respected. The model described by equations (1)-(6) was implemented in Matlab.

$$|q| \leq \left|-K(h)\left(\frac{\partial h}{\partial z}+1\right)\right| \quad \text{(Eq. 6)}$$

First, the reference evapotranspiration (ETo) was determined with FAO Penman-Monteith equation (Allen et al. 1998). After that, the potential evapotranspiration (ETp) was estimated from reference evapotranspiration (ETo), using the dual crop coefficient approach (Allen et al. 1998), with one coefficient for crop transpiration (Kcb) and another coefficient for soil water evaporation (Ke). Crop potential transpiration was estimated for each day as a function of plant development, and soil water evaporation is a function of wetness and soil surface covering (Allen et al. 1998). Both, crop transpiration and soil water evaporation coefficients are estimated for each crop stage (i.e. initial, crop development, mid-season, and late season) (Rosa et al. 2012).

Soil water evaporation was estimated as defined in (Allen et al. 1998, 2005) using the parameters which allowed the computation of total and readily available soil water (TAW and RAW, mm), as well as the initial values for the total evaporable water (TEW, mm), readily evaporable water (REW, mm), and thickness of the evaporation soil layer (Ze, m). Soil water evaporation coefficient (Ke) represents the contribution of evaporation from soil to total evapotranspiration (Pereira et al. 2015). Calculation of soil water evaporation coefficient (Ke)

uses a variation of the second stage of Ritchie's soil evaporation approach (Ritchie 1972) described in details by Allen et al. (1998, 2005).

Root water uptake was simulated using the model proposed by de Jong van Lier et al. (2008) (Eq. 7), that used the root length density and matric flux potential of each soil layer (Eq. 8). This model was coupled with the Richards' equation in one-dimensional (1D) by water uptake model (Eq. 7). The matric flux potential (*M*, $cm^2\ d^{-1}$) is defined as the integral of unsaturated hydraulic conductivity, (K(h), $cm\ d^{-1}$), over pressure head (*h*); or equivalently as the integral of diffusivity, (*D*(θ), $cm^2\ d^{-1}$), over water content (θ, $cm^3\ cm^{-3}$) (de Jong van Lier et al. 2008). The low bound of the integral is the permanent wilting point in terms of pressure head (h_w, cm) or water content (θ_w, $cm^3\ cm^{-3}$).

$$S_z = \rho_z\left(M(h)_z - M_{0,z}\right) \qquad \text{(Eq. 7)}$$

where ρ_z (cm^{-2}) is defined as weighting factor for matric-flux potential dependent of root uptake; M(h) is the matric flux potential ($cm^2\ day^{-1}$); M_0 is the matric flux potential at the root surface ($cm^2\ day^{-1}$). The matric flux popential is given by

$$M(h) = \int_{h_w}^{h} K(h)\partial h = \int_{\theta_w}^{\theta} D(\theta)\partial\theta, \qquad \text{(Eq. 8)}$$

where h is the pressure head (cm); h_w is the pressure head at the wilting point (cm); K is the unsaturated hydraulic conductivity ($cm\ day^{-1}$); D is the diffusivity ($cm^2\ day^{-1}$); θ is the soil water content ($cm^3\ cm^{-3}$); θ_w is the water content at the wilting point.

The procedure for calculating root water uptake (Eq. 7) was described by de Jong van Lier et al. (2008) and estimated the water uptake for each layer dependent on the matric flux potential (Eq. 8) with a reduction function for root length density, given by

$$\rho_z = \frac{4}{r_{o,z}{}^2 - a_z{}^2 r_{m,z}{}^2 + 2\left(r_{m,z}{}^2 + r_{o,z}{}^2\right) ln\left(a_z r_{m,z} / r_{0,z}\right)}, \qquad \text{(Eq. 9)}$$

in which ρ_z (cm^{-2}) is a weighting factor for matric-flux potential dependent of root uptake; a_z is a constant equal to 0.53; z is the soil layer (cm); $r_{0,z}$ is the root radius (cm); and $r_{m,z}$ is the half-mean distance between roots (cm) which can be computed from the root length density according to Eq. 10 (de Jong van Lier et al. 2008).

$$RLD = \frac{1}{\pi . r_m^2} \quad \text{or} \quad r_{m,z} = \sqrt{\frac{1}{\pi . RLD}}, \qquad \text{(Eq. 10)}$$

where RLD is the root length density ($cm\ cm^{-3}$); r_m is the half-mean distance between roots (cm); z is the each soil layer (cm). The half-mean distance between roots is a measure for the soil volume each root can exploit to water uptake.

The root radius ($r_{0,z}$) and root length density are simulated from input parameters with the equations from the RootBox model (Leitner et al. 2010b).

Actual transpiration (T_a) cannot be higher than the potential transpiration (T_P, $cm\ day^{-1}$) of the plant. Actual transpiration is given by the integral of water uptake (Eq. 7), resulting in Eq. (11). The matric flux potential M_0 is initially considered equal to zero, i.e., $h = h_w$ at the root surface, but if the obtained transpiration is larger than potential transpiration, no water stress occurs and thus M_0 is larger than zero and its value is obtained by setting $T = T_P$ (Tron et al. 2015).

$$T_a = \int_0^{z_{max}} S_{(z)}\, dz \qquad \text{(Eq. 11)}$$

where T_a is actual transpiration ($cm\ day^{-1}$); z_{max} is the maximum root depth (cm); $S_{(z)}$ is the water uptake in each soil layer ($cm\ day^{-1}$).

Calibration of soil strength function

Soil penetration resistance varies greatly with soil water status, and was modelled as a function of soil water content and bulk density using a non-linear model (Eq. 12) (Busscher 1990). In equation 12 the constants (*a, b,* and *c*) are found by empirically fitting to the experimental values of soil penetration resistance, water content and bulk density (Moraes et al. 2017). In this paper a soil penetration resistance function was used for a data set measured in the laboratory for a Rhodic Eutrudox (Ortigara et al. 2015). The relation between predicted and measured penetration resistances simulated are distributed closely around the one-to-one line in Fig. 3, with a correlation coefficient of 0.91. Thus, Busscher's model (Eq. 12) can be used to describe soil penetration resistance for this soil, given by

$$Q_p = a\,\gamma^b\theta^c \qquad \text{(Eq. 12)}$$

where Q_p (MPa) is the soil penetration resistance; γ (Mg m^{-3}) is the dry bulk density; θ (cm^3 cm^{-3}) is volumetric soil water content and *a, b* and *c* are empirical parameters.

Root stress function: Root elongation as a function of soil physical stresses

Root elongation is a function of soil strength and matric potential (Fig. 4a,b), and for simplicity we assume that these stresses combine linearly i.e. the stresses act independently to decrease elongation rate. This results in a relation where root elongation rate is defined for all combinations of penetration resistance and matric potential, and so can be used to produce a heat-map where red indicates slow root elongation due to physical stress, and blue indicates unimpeded root growth (Fig. 4c,d).

The heat-map therefore represents the response of a particular plant genotype to soil physical stresses. By plotting the penetration resistance as a function of soil matric potential on the same diagram, the effect of soil physical stress on root elongation is represented for the range of water contents that the plant may experience during the growth season (eg. see plotted points on Fig. 4c, representing two soil compaction levels). If the soil is moist at the start of the growth season, root elongation will be in the blue zone and relatively fast. As the soil dries (e.g. during a period with little rain), the soil strength will increase and the elongation rate will slow – much faster in the case of the upper strength characteristic curve (hollow circles in Fig. 4c), than for the more benign soil (shaded squares in Fig. 4c). Thus, this heat-map diagram can be used to capture many elements of the complex interactions that occur between contrasting soil types, management regimes, climate and plant genotype. By interpreting this diagram with weather data for a particular year, it can be used to compare stresses that limit root elongation in different seasons.

One aspect that is difficult to represent is the increased root elongation due to continuous macropores. Whilst it is not possible to represent this phenomenon mechanistically without detailed root-tip scale modelling of the soil structure, we have sought to heuristically adjust the root growth function to permit faster elongation at the same penetrometer resistance in soil containing macropore channels (Fig. 4d). Our justification for this is that root growth has been observed in these Brazilian field soils with very large penetration resistances in a depth, where root growth would not normally be expected.

In the next two sections we describe the root model, the relation to the soil physical stresses, i.e. water stress and hypoxia, and penetration resistance.

Root elongation under water stress and poor aeration

Using the Feddes concept for water uptake (Feddes et al. 1978), and adapting for root elongation yields

$$\mathrm{RE(h)} = \alpha(\mathrm{h})\mathrm{RE}_{\max}\,, \qquad \text{(Eq. 13)}$$

where RE(h) is the root elongation potential affected by matric potential (cm day^{-1}), α_h is a dimensionless prescribes function of soil water pressure head and, RE_{max} (cm day^{-1}) is the maximal possible root elongation without restrictions.

Under non-optimal conditions, i.e. either too dry (water deficit) or too wet (poor aeration), the root elongation is reduced by means of the stress reduction factor (α(h)) from 1 (maximum root elongation) to zero (no growth). The shape of this function for root elongation follow the concept proposed to by Feddes et al. (1978) (Eq. 14). We used four limits of matric potential (h), i.e., that there is a linear increment of root growth from h_1 (-0.1 kPa) to h_2 (-6 kPa), and a linear reduction of the root elongation from h_3 (-10 kPa) to h_4 (-1000 kPa). The h_1 was defined at the wet end and represents the start of water drainage and increase of soil aeration (and oxygen concentration) necessary for root growth (Dresbøll et al. 2013). The h_2 and h_3 are the values close to field capacity (Iijima and Kato 2007), when there is no water stress and thus root elongation rate is at its maximum. The value h_3 was defined as the limit of maximum growth due to turgor pressure in the expanding cells of the root elongation zone, and is typically up to 1 MPa (Bengough et al. 2011). The equation is given by

$$\alpha(\mathrm{h}) = \begin{cases} 0 & \text{if} \quad |\mathrm{h}| \le |\mathrm{h}_1| \\ \dfrac{(|\mathrm{h}_1| - |\mathrm{h}|)}{(|\mathrm{h}_1| - |\mathrm{h}_2|)} & \text{if} \quad |\mathrm{h}_1| < |\mathrm{h}| \le |\mathrm{h}_2| \\ 1 & \text{if} \quad |\mathrm{h}_2| < |\mathrm{h}| \le |\mathrm{h}_3| \\ \dfrac{(|\mathrm{h}_4| - |\mathrm{h}|)}{(|\mathrm{h}_4| - |\mathrm{h}_3|)} & \text{if} \quad |\mathrm{h}_3| < |\mathrm{h}| \le |\mathrm{h}_4| \\ 0 & \text{if} \quad |\mathrm{h}| > |\mathrm{h}_4| \end{cases} \qquad \text{(Eq. 14)}$$

where α(h) is the stress reduction factor of root elongation due pressure head; |h| is the module of pressure head, and h_1, h_2, h_3 and h_4 are the limits of pressures head for root elongation (Fig. 4a). Root elongation below $|h_1|$ (critical respiratory oxygen pressure, with $|h_1|$ approaching to saturation (1 cm) (Saglio et al. 1984)) and above $|h_4|$ (maximum growth pressure, with $|h_4|$ approaching 1 MPa (Bengough et al. 2011)) is set equal to zero. Between $|h_2|$ and $|h_3|$ (reduction point, $|h_2|$ is 6 kPa, and $|h_3|$ is 10 kPa) root elongation is maximal. Between $|h_1|$ and $|h_2|$ and between $|h_3|$ and $|h_4|$ a linear variation is assumed.

Root elongation in relation to soil strength

The effects of water stress, poor aeration, and soil strength on root elongation (Eq. 15), can be predicted from the stress reduction function Eq. (16) and is shown in Fig. 4c and Fig. 4d. The root elongation rate can slow due to soil strength, with an exponential decrease for a soil without continuous macropores (Eq. 17) (Bengough 1997). Thus, root elongation can be represented as a function of soil strength (Q_p) and matric potential (h), at time (t) and depth (z) (Eq. 15). The stress reduction function in a layer z, on day t shows the effect of field conditions on root elongation (Eq. 16). Biopore effects on facilitating root elongation are included very simply in the root model by changing the relationship between root elongation rate and soil strength (Eq. 18), as indicated by the blue dashed line at the Fig. 4b (Bengough 2012; Jin et al. 2013). This favours faster root elongation, and changes the root response to soil strength. The predicted rate of root elongation is therefore relatively faster in soil containing many biopores, as compared with one containing few biopores, at the same penetration resistance (Fig. 4d compared with Fig. 4c).

$$\mathrm{RE}\left(Q_p, \mathrm{h}\right)_{t,z} = \mathrm{srf}\left(\mathrm{Q}_p, \mathrm{h}\right)_{\mathrm{t,z}} \mathrm{RE}_{\max} \qquad \text{(Eq. 15)}$$

$$\mathrm{srf}\left(\mathrm{Q}_p, \mathrm{h}\right)_{t,z} = \alpha\left(Q_p\right)_{t,z} \alpha(\mathrm{h})_{t,z} \qquad \text{(Eq. 16)}$$

where $\mathrm{srf}\left(\mathrm{Q}_p, \mathrm{h}\right)_{t,z}$ is the total stress reduction function for root elongation due to mechanical (Q_p) and hydric (h) stresses in each time (t) and depth (z); α(Q_p) is the stress reduction function by soil strength and is given by Eq. (17) in a soil without continuous macropores or by Eq. (16) for a soil with continuous macropores; α(h) is the stress reduction function by matric potential

(water and aeration stress) and, t is the time (day), z is the depth (cm); RE_{max} is the root elongation maximal possible without restrictions (cm day^{-1}), and RE is the root elongation (cm day^{-1}).

$$\alpha(Q_p) = \exp(-0.4325\ Q_p), \quad \text{(Eq. 17)}$$

$$\alpha(Q_p) = \exp(-0.30\ Q_p), \quad \text{(Eq. 18)}$$

Note that we make the assumption that the combined effect (Eq. 16) of the two stresses (mechanical and hydric) is multiplicative for each time and depth. In addition, penetrometer resistance that depends on water content and bulk density is used as the measure of soil strength.

Coupling of the model

The link between root and soil water models is the water uptake (1D sink term) in Richards' equation (Tron et al. 2015), and the link for soil physical conditions and root growth is the stress reduction function for root elongation (Fig. 6). The sink term represents root water uptake from each horizontal soil layer (1 cm thick), and soil physical conditions control the stress reduction function that restricts root elongation and root system growth. The water uptake term depends on two factors: root length density and availability of water in each soil layer (de Jong van Lier et al. 2008). Thus, the model is dynamic: e.g. where there are more roots for water uptake, the soil may become dry and hard, with greater restriction to root elongation. However, the effects on root elongation act on each single root, which can ultimately influence the root system architecture.

Implementation and parameterization

The root growth model was implemented by extending the L-system model for root growth, RootBox (Leitner et al. 2010a), and is written in Matlab®. The water flow in soil was implemented into Rootbox as described in Tron et al. (2015). Water flux, soil physical conditions, and the stress reduction function for root elongation and root growth are alternately computed at each time step, which was set to be 1 day. Each segment root was submitted to dynamic soil physical conditions in a specific day and position from a soil layer with 1 cm depth layer resolution.

Model parameters are: (1) parameters describing the soil (soil water retention curve, soil penetration resistance curve and bulk density) (e.g., Table 1), (2) parameters regarding climate (potential evaporation and transpiration, temperature, air humidity, rainfall and irrigation), and (3) root architecture parameters (i.e., initial root elongation, length of the apical and basal zone, spacing between branches, number of branches and insertion angle), type of tropism, growing period and limits for root elongation) (e.g., Table 2).

Model output parameters are related to the soil conditions (water balance, infiltration, runoff and deep drainage, actual evaporation rate, water content, matric potential, soil penetration resistance and unsaturated hydraulic conductivity) and crop root system structure, root length density, actual transpiration and water uptake at each layer.

Simulation scenarios

Calibration of soil strength function against field data of soil water content and soil penetrometer resistance

The model was tested using soil physical parameters (Table 1), soil water content and soil penetration resistance of a Rhodic Eutrudox in a no-tillage system (Moraes et al. 2012, 2013). In this experiment, there was no plant growth, but the accuracy of the Richards' equation was evaluated. Data of water content and soil penetration resistance of two soil layers (0-10 cm and 10-20 cm depth) from a field experiment were obtained from 45 days in a wet-dry cycle on field conditions carried out at the Embrapa Soybean experimental station at Londrina, Brazil.

Simulation case study: effects of a compacted layer on root growth

We simulated the root growth of soybean for 87 days, from 10th October 2013 (sowing) to 5th January 2014 (sample roots). Two soil conditions were simulated in order to analyse the reduction of root elongation rate due to soil compaction, no-tillage without or with a compact soil layer from 16 to 20 cm depth. The bulk density in the soil profile (0-100 cm depth) for loose soil was 1.0 Mg m^{-3}, using the same profile but with a compacted soil layer, from 16 to 20 cm of bulk density of 1.30 Mg m^{-3}.

For the simulation we used the daily time series of climate data from Embrapa Soybean experimental station, in Londrina (latitude 23º11'S; longitude 51º11'W; and 620 m altitude), State of Paraná, southern Brazil (Fig. 5). The simulation was made using the soil physical properties (Table 1) of an Oxisol (Latossolo Vermelho Distroférrico, in Brazilian classification; and Rhodic Eutrudox, in USA classification) on no-tillage system (established in 1997) with 755 g kg^{-1} of clay, 178 g kg^{-1} of silt and 67 g kg^{-1} of sand.

Field experiment comparison: typical versus drought seasons

For the simulation we used: the daily time series of climate data from two growing seasons at Embrapa Soja, in Londrina (latitude 23º11'S; longitude 51º11'W; and 620 m altitude), State of Paraná, southern Brazil (Fig. 11); the soil physical properties of an Oxisol (Latossolo Vermelho Distroférrico, Brazilian classification; Rhodic Eutrudox, USA classification) on a no-tillage system (established in 1997) with 755 g kg^{-1} of clay, 178 g kg^{-1} of silt and 67 g kg^{-1} of sand (Table 1). Two season growth conditions were used to compare the effects of weather, a drought (2008/09) and a wet (2009/10) season on root development (Franchini et al. 2017). The parameters used to calculated the plant transpiration, soil evaporation and crop growth stages are summarized in Table 3.

Soybean root system development (Cultivar BRS-282) was simulated for 70 days, for both wet and drought seasons. For the drought season, the soybean was seeded on 24th November 2008, with roots sampled from the field on 2nd February 2009 (Franchini et al. 2017). The main time with water stress in drought season was during the first 54 days after sowing, that was used to identify the drought stress on root growth. In the wet season, soybean root growth season was simulated from 12th November 2009 to 20th January 2010 (Franchini et al. 2017) for one individual plant. After that, the root length densities were converted to a per-area basis and in 1D assuming the area of each plant with a population of 30 plants m^{-2}, with 0.45 cm inter-rows, i.e., 7 cm inter-plants in the row. Soil water flux was simulated to 100 cm depth. Root elongation was modelled daily incorporating the effects of soil and climate conditions. Root length density and root system architecture were simulated for 70 days. Results were compared with both root length density and an excavated profile wall in the field.

Statistical evaluation of model performance

The agreement between simulated and measured values was expressed by the mean absolute error (MAE) (Eq. 19) (Casaroli et al. 2010), the root mean squared error (RMSE) (Eq. 20) (de Jong van Lier et al. 2008), the coefficient of residual mass (CRM) (Eq. 21), the coefficient of correlation (r) (Eq. 22) (Bonfante et al. 2010), and the index of agreement (d) (Eq. 23) (Casaroli et al. 2010). Also, the modelling efficiency (EF) (Eq. 24) (Bonfante et al. 2010), and the one-to-one line were used as criteria to evaluate the model performance.

$$MAE = \frac{1}{n}\sum_{i=1}^{n} |P_i - O_i| \qquad \text{(Eq. 19)}$$

where n is the total number of measurements, O_i and P_i are the measured and predicted values of the observation, respectively. The root mean square error (RMSE) has minimum and optimum value at 0. It is a difference-based measure of the model performance in a quadratic form, and it is sensitive to outliers.

$$RMSE = \sqrt{\frac{1}{n}\sum_{i=1}^{n}(P_i - O_i)^2} \quad \text{(Eq. 20)}$$

The coefficient of residual mass (CRM), ranges between −∞ and +∞, with the optimum equal to zero. Positive values indicates that the model underestimates the prediction, and negative values indicates overestimation. When CRM are close to zero it indicates the absence of trends.

$$CRM = \frac{\sum_{i=1}^{n} Oi - \sum_{i=1}^{n} Pi}{\sum_{i=1}^{n} Oi} \quad \text{(Eq. 21)}$$

The optimum value of the coefficient of correlation (r) (Addiscott and Whitmore 1987) is equal to 1; zero means no correlation.

$$r = \frac{\sigma OP}{\sigma O.\sigma P} \quad \text{(Eq. 22)}$$

where σOP is the covariance between measured and estimated data and σO and σP are the measured and estimated standard deviation, respectively.

The index of agreement of Willmott (d) is dimensionless, lies between −1.0 and 1.0, and is more related to model accuracy than other indices (Willmott et al. 2012).

$$d = 1 - \frac{\sum_{i=1}^{n}(P_i - Oi)^2}{\sum_{i=1}^{n}(|P_i - \bar{O}| + |Oi - \bar{O}|)^2} \quad \text{(Eq. 23)}$$

Modelling efficiency (EF) (Greenwood et al. 1985) can get either positive or negative values, 1 being the upper limit, while negative infinity is the theoretical lower boundary. EF values lower than 0 result from a worse fit than the average of measurements.

$$EF = \frac{\sum_{i=1}^{n}(O_i - \bar{O})^2 - \sum_{i=1}^{n}(P_i - O_i)^2}{\sum_{i=1}^{n}(O_i - \bar{O})^2} \quad \text{(Eq. 24)}$$

Results

Soil water content and soil penetration resistance in a soil without roots

Simulated soil water content was plotted against measured soil water content at 8 cm and 16 cm depths in the Rhodic Eutrudox no-tillage treatment, in the absence of a crop during a wet-dry cycle (Fig. 6a). Simulated penetrometer resistances were similarly compared with field measurements at the same two depths (Fig. 6b). The simulations using weather and soil data resulted in good prediction of soil water content and penetration resistance, with points lying close to the 1:1 line (Fig. 6a and Fig. 6b). The linear regression lines for simulated and measured data of soil water content or penetration resistance were not significantly different from the 1:1 lines at 95% confidence level. The index of agreement (d) was 0.84 for water content, with correlation coefficient (r) of 0.86 (Fig. 6a). Simulated and measured values of soil penetration resistance were in very good agreement (index of agreement 0.92, correlation coefficient 0.85; Fig. 6b). This suggests that the relevant processes were captured in the model. Prediction of soil water content and penetrometer resistance was appropriate for Rhodic Eutrudox soil.

The proposed model offers a useful framework to investigate the effects of soil physical conditions on root growth and the stress reduction function can be used as input for other soil-plant models.

573 **Simulation case study: effects of a compacted layer on root growth**
574

575 The same climate data were used for the 87 day root growth simulation (see
576 Supplementary videos S1 and S2). Total precipitation was 352 mm, during 31 days of rain.
577 Simulations of the soybean root system are shown with (Fig. 7a and supplementary video S1)
578 and without the presence of a compact layer (Fig. 7b and supplementary video S2). The stress
579 reduction factor is plotted as a function of time and depth for these two soil conditions, adjacent
580 to the root simulations (Fig. 7e and Fig. 7f): darker blue indicates more rapid root elongation,
581 whilst red indicates a large decrease in root elongation due to soil physical stress.
582 The root distribution was much more uniformly tapering for the profile without a compact
583 zone (Fig. 7a). Many main root axes penetrated below 16 cm depth, and lateral roots
584 proliferated freely around these axes. The tap root spends 9 days more to cross compacted soil
585 layer (16-20 cm depth) compared to the uncompacted soil (Fig. 7c,d). The stress reduction
586 function indicated relatively little decrease in root elongation rates until day 60, when elongation
587 slowed in the surface layers, the root system extended down to 70cm by day 70.
588 In the presence of a compact layer, the pattern of root growth was changed, with a
589 corresponding alteration of root distribution down the soil profile. Fewer main root axes crossed
590 the compact soil layer from 16 to 20 cm depth, and there was a noticeable gap in lateral root
591 proliferation in the compact zone. Root length density in the compacted soil layer (16-20 cm)
592 was reduced 83 %, from 0.90 cm cm^{-3} (compacted soil) to 0.15 cm cm^{-3} (uncompacted soil).
593 However, root length density in the layers (0-15 cm depth) above the compacted layer was
594 increased 25 % to 1.25 cm cm^{-3} (compacted soil) from 0.99 cm cm^{-3} (uncompacted soil) (Fig.
595 7c,d). The stress reduction function indicated that root elongation rates in the compact layer
596 were typically slowed to below 20% of the maximum root elongation rate – a very substantial
597 impediment to root elongation – although the main tap root still penetrated below 75 cm depth
598 by day 70.
599 The effect of a compact layer in the soil profile changed root architecture and root length
600 density distribution; however, rooting depth was similar in both soil conditions, to a maximum of
601 75 cm depth. The thin 5 cm compact layer substantially altered the water uptake pattern (Fig.
602 8b), mainly due to the restriction on root system development (Fig. 7b). Water uptake was
603 localised where the root length density was greatest adjacent to plant-available water, as
604 modelled by matric flux density (de Jong van Lier et al. 2008). In the compacted-layer scenario,
605 the root system (and water uptake) was restricted to shallower than 20 cm depth for 20 days
606 (Fig. 8b). However, by 20 days in the scenario with loose soil (free of compact layer), the root
607 system was already extracting water to 40 cm (Fig. 8a). The water uptake was generally higher
608 in the uncompacted scenario in the top 15 cm of soil until 65 days of plant growth, due to the
609 more superficial proliferation of the root system as compared with the uncompacted profile.
610 To understand which factors influenced the root elongation most, it is necessary to further
611 analyse the stress reduction factor parameter. Soil penetration resistance and water content
612 both varied substantially during the growth season (Fig. 9). Soil penetration resistance was
613 changed over time (Fig. 9a,b) due to water flux in the soil (Fig. 9c,d). Within the compacted soil
614 layer this lead to a soil penetration resistance that was higher than 4 MPa, acting as a limitation
615 to root elongation. Soil water content was changed during the growth season due to crop water
616 uptake or soil water movement (due to water evaporation, deep drainage, etc.). As expected,
617 the rooting depth developed faster in loose soil than in the soil including the compacted layer.
618 The root system under soil compaction was delayed, limiting the water available to root water
619 uptake from deeper layers and therefore plant transpiration. Faster root growth in loose soil
620 favours root system water uptake, and quickly depletes soil water over the soil profile. This
621 increases the penetration resistance which limits root elongation.
622 Fig 10. shows the effects on root elongation modelled by the stress reduction function for
623 the modal values of 0.73 in the loose soil and 0.14 in the soil with a compacted soil layer(Fig.
624 10a). The separation of the total stress reduction functions into two effects, one of penetration
625 resistance (Fig. 10b) and the other of matric potential (Fig. 10c), favour to analyse the relative
626 distribution of the stress reduction factor values that reduce the root growth of soybean. The
627 reduction factor associated with high soil penetration resistance was closer to zero (high
628 restriction) for the soil with a compact layer with modal value of 0.15 (Fig. 10b) in contrast to a
629 modal value of 0.76 in the uncompacted soil (Fig. 10b). Restrictions of root elongation due to
630 matric potential were similar for both soil conditions (Fig. 10c), with modal values of 0.93 (loose
631 soil) and 0.94 (soil with a compacted layer). This indicates that mechanical impedance (Fig.
632 10b) exerted a greater limitation to root elongation in soil with a compacted layer (Fig. 10a).

633
634
635 **Field experiment comparison: typical versus drought seasons**
636
637 In this section, comparisons between simulations and field experiments are reported
638 showing simulated root system architecture, root length density distribution, stress reduction
639 factor, and water uptake distribution. The simulations are then compared with measurements of
640 root length density distribution and excavated profile walls of soybean plants grown in the field
641 during the two seasons.
642 During the drought season 2008/09, it rained 306 mm during 70 days of root growth, with
643 32 of these days having rainfall (Fig. 11a). During the wetter season of 2009/10, there were 46
644 days with rainfall, giving a total of 515 mm rainfall (Fig. 11b). During the first 54 days in 2008/09,
645 there was only 131 mm (2.4 mm day^{-1}) of rainfall compared to 354 mm (6.5 mm day^{-1}) of rainfall
646 in the same period in 2009/10 (Fig. 11). The rainfall distribution was irregular in the drought
647 season affecting root development, and was associated with large penetration resistance values
648 in the field (Moraes et al. 2013).
649 The simulated stress reduction function limited root elongation in the dry season, with
650 corresponding changes in simulated root architecture and root length density distribution (Fig.
651 12 and see Supplementary videos S3 and S4). The simulated root system grew slower,
652 especially early in the dry season (see supplementary video S3). Reduced rainfall quantity in
653 2008/09 increased the hydric and mechanical stress to root growth. Rooting depth in 2008/09
654 was 52 cm after 54 days and 48% smaller than rooting depth in 2009/10 in the same period (77
655 cm depth). During this period the root length density was reduced for 46% (from 0.41 cm cm^{-3} to
656 0.28 cm cm^{-3}, for 2009/10 and 2008/09 respectively) in the first 30 cm depth (Fig. 12). Both the
657 depth of and the volume of soil explored by the simulated root system during the drought
658 season (2008/09) was decreased in relation to the wet season (2009/10).
659 The distribution of the total stress reduction function differed between wet and dry
660 seasons (Fig. 13). The relative frequency of total stress indicates that 76 % of the values were
661 smaller than 0.4 (yielding a reduction of 60% in root elongation rate) in dry season. However, in
662 wet season it was only 36 % of total stress values. Stress from mechanical impedance
663 contributed to a reduction higher than 60 % of root elongation rate in 70 % of the cases. In
664 contrast, in the wet season root elongation was reduced only in 29 % of the cases. Stress from
665 matric potential to root elongation smaller than 0.90 was increased from 9 % to 42 % of values
666 in the wet and dry season, respectively (Fig. 13). The frequency of stress reduction over rooting
667 depth during the first 54 days (major rainfall deficit in 2008 season growth) showed that the
668 main stress limiting root elongation was due to soil penetration resistance in the wet season. In
669 the drought season, root elongation was also reduced due to hydric stress (42 % cases with
670 values smaller than 0.9), which was less in the wet season (9 % of the cases). The modelling
671 results suggest that in this soil during a dry season, mechanical impedance became a major
672 limitation to root elongation. In the drought season, roots experienced more days of soil physical
673 stress (Fig. 13a), with a combination of penetration resistance (stress reduction factor <0.4)
674 (Fig, 13b) and matric potential (stress reduction factor<0.9) limiting root elongation (Fig, 13c).
675 Water uptake rate and distribution differed substantially between wet and dry seasons
676 (Fig. 14). During the first 54 days in drought season (2008/09) soybean took up 51 mm (i.e.
677 denoted mm= litre m^{-2}) of water depth, which is only 50% of the water uptake in the wet season
678 (2009/10), in the same period (see Fig. 14). In the dry season, the root system extended to
679 depth more slowly, resulting in a slower spread of the water extraction volume in depth. Plants
680 were submitted to greater stress under drought with an associated decrease in transpiration.
681 Simulated and measured root length density was very similar for all layers at the soil profile for
682 both weather conditions (Fig. 15 and Fig. 16). There was qualitative agreement between the
683 model predictions and field observations of root length density for all soil profile (Fig. 16c).
684 Indicators describing the model quality were promising: modelling efficiency (EF) 0.87, index of
685 agreement (d) 0.97, RMSE 0.10, coefficient of residual mass 0.0061, coefficient of correlation
686 0.83, and means absolute error 0.08. The values indicate a good agreement between measured
687 and simulated values (Fig. 16c).
688
689
690 **Discussion**
691

692 Few studies have published comparisons between root elongation and soil physical
693 conditions (Bengough et al. 2011). Even in the most commonly studied crops, such as soybean
694 (Gregory 2006), maize (Schmidt et al. 2013), pea (Iijima and Kato 2007) or cotton (Taylor and
695 Ratliff 1969), there is still a lack in investigating the combined effect of soil physical stresses of
696 hypoxia, water deficit and mechanical impedance (Bengough et al. 2011). In this paper, we
697 assumed that stresses from soil physical conditions reduce the root elongation as a combined
698 effect as described in Bengough et al. (2011). Root elongation parameters (Fig. 4) should be
699 similar for different soils or crops (Iijima and Kato 2007), because they are a generic response
700 of root elongation to matric potential (Fig. 4a) and mechanical impedance (Fig. 4b). We used
701 the relationship of root elongation and penetrometer impedance from Bengough (1997). We
702 expect the same relationship between the stress reduction function (that is dimensionless
703 quantity, from zero to one) and the soil physical conditions (e.g. Iijima and Kato (2007)),
704 furthermore the differences between crops should be only in the range of the elongation rate.
705 We presented the root system parameters used in our modelling case study (Table 2), including
706 the initial tip elongation rate (5.5 cm day^{-1}) for unimpeded conditions. We calibrated the model
707 with field data from soybean root growth in no-tillage system at two weather conditions (Fig. 16).
708 We compared root length density modelled and measured in the field (Fig. 15 and 16) to include
709 the effect of continues pores and biopores (Fig. 4d) in no-tillage system (Moraes et al. 2016) to
710 reduce the mechanical impedance to root elongation (Bengough 2012; Jin et al. 2013) as
711 showed that changes in the relationship of root resistance and penetrometer resistance (Fig.
712 4b) due presence of biopores or crack in the soil profile (Bengough and Mullins 1991).
713 Root water uptake depends on soil water status, soil hydraulic properties, root length
714 density, and root radius (de Jong van Lier et al. 2013). In this work, we propose a new
715 modelling approach for root architecture development as affected by soil physical stresses and
716 its effect of root water uptake. We demonstrate that it well represents the root growth of
717 soybean growing in compacted soils. Soil strength and water availability can, independently,
718 reduce crop growth but there is no consensus on which of these stresses or combination of
719 stresses is the most important (Jin et al. 2013). By separating the total stress reduction function
720 for root elongation into two effects, one being the penetration resistance and the other one the
721 matric potential, we could analyse the relative contribution of the different stresses to the overall
722 reduction factor values. The effect of matric potential on root elongation restriction was similar in
723 two different soil conditions, with and without a compact layer. However, the relative frequency
724 of mechanical stress on root elongation was found from 0.70 to 0.90 in the loose soil, while the
725 stress values in the soil with a compact layer ranged from 0.00 to 0.30, indicating that
726 mechanical impedance exerted a greater limitation to root elongation in this case.
727 Rooting depth in both soil with or without a compacted layer were similar. However, root
728 system development was slower in the soil including the compact layer, leading to a reduced
729 root length density within this layer. Drought stress adversely affects plant growth by decreasing
730 the uptake of water and nutrients by plants (Miransari 2016a). Root length density was
731 decreased into the soil compacted layer due mechanical impedance (Bengough et al. 2011),
732 water stress (Benjamin and Nielsen 2006) and poor aeration (Valentine et al. 2012). The
733 strongest influence on root elongation in compacted soil is due to soil strength. Furthermore, the
734 combined effect of mechanical impedance and oxygen deficiency (hypoxia) impedes root
735 development (Valentine et al. 2012). Under compaction the root growth is adversely affected, as
736 the soil structure will not be suitable for root growth (Miransari 2016b).
737 Our new model considers the mechanical and hydric stresses for each root to elongation
738 over time (e.g. Fig. 12e and 12f) including root water uptake and soil water flux daily at soil
739 profile (e.g. Fig. 14). This was the first time that the soil physical conditions (mechanical and
740 hydric stresses to root elongation) were included into a root growth model; before that the
741 RootBox model (Fig. 12e and 12f) only predicted root growth due to time (root age) or due to
742 different types of tropisms such as chemotropism. In relation to other models, for example,
743 Hydrus (Hartmann and Šimůnek 2016; Hartmann et al. 2017) or SWAP (Kroes et al. 2008)
744 models have a root growth package, however, those models do not consider the soil physical
745 conditions for each single root and do not consider the 3D root architecture.
746 In addition, there are few three-dimensional root architectural models actually in use, in
747 summary the most common and current models include RootTyp (Pagès et al. 2004), SimRoot
748 (Lynch et al. 1997), ROOTMAP (Diggle 1988b, a), SPACSYS (Wu et al. 2007), R-SWMS
749 (Javaux et al. 2008), Archisimple (Pagès et al. 2014), OpenSimroot (Postma et al. 2017),
750 RootBox (Leitner et al. 2010a, b), and CrootBox (Schnepf et al. 2017) which have been used for
751 a range of root modelling studies (Dunbabin et al. 2013). An advantage of RootBox (Leitner et

al. 2010a) over other models is that it is implemented in Matlab in a way that keeps it open for any changes to the model structure (Dunbabin et al. 2013). Soil mechanic impedance effects on root growth is used only in SPACSYS (Wu et al. 2007), R-SWMS (Clausnitzer and Hopmans 1994; Javaux et al. 2008), and HYDRUS (Hartmann et al. 2017); however, the strength of stress is determined from empirical relationships between mechanical stress and bulk density, texture (only sand content) and water content (Jones et al. 1991). Thus, for each soil we should fit the relationship of soil penetration resistance, water content and bulk density (Busscher 1990) to know the mechanical impedance over time. Those equations from Jones et al. (1991) do not represent the correct relationship of soil penetration resistance with water content and bulk density (Busscher 1990), especially when affected by soil structure (Moraes et al. 2017) in clayey soils (Moraes et al. 2012), as described in this paper. In addition, the root growth module of the HYDRUS model (Hartmann et al. 2017) uses environmental stresses such as temperature, aeration, and chemical soil condition (Al toxicity and Ca deficiency) to reduce the root system growth. Environmental stresses are calculated as a function of sand content and soil moisture (Jones et al. 1991), and affect rooting depth and root proliferation within different soil layers (Hartmann et al. 2017). Thus, that effect is very generic and does not consider each individual root within the root system as detailed as in the RootBox model (Leitner et al. 2010a).

The new root architecture model can simulate the stress (mechanical and hydric) of each individual root (tap root, lateral and secondary roots) in each position in the soil profile. We include the root water uptake model due matric flux potential as a function of the distance to the root (de Jong van Lier et al. 2008); the model includes compensation mechanisms such that reductions in the uptake from dry layers are compensated by an increase in the uptake from wetter layers. We are not creating a new water uptake model, but use a physically based root water uptake model with an implicit compensation mechanism which has been validated by de Jong van Lier et al. (2008). Also, this model has been tested in others studies (e.g. de Jong van Lier et al. (2008), Casaroli et al. (2010) and Tron et al. (2015)). As described in the original model, this water uptake model is based on an expression for the matric flux potential as a function of the distance to the root, and assuming a depth-independent value of matric flux potential at the root surface, uptake per layer (de Jong van Lier et al. 2008). The weighting factor for root water uptake depth distribution that depends on root length density and root radius (de Jong van Lier et al. 2008) is calculated by the RootBox model as result of soil physical conditions.

Our soil-plant-atmosphere model simulated dynamic effects of soil stresses on root growth and root water uptake by alternating the root growth and soil water flow model at a coupling time step of 1 day. However, we could not sample daily fluctuation of root growth in the field experiment; we sampled at the end of the crop season for measurement of total root growth and stress limitation that the root system was submitted to during the cropping season. The simulated root length density agreed with measured field data (Fig. 16). This indicates that the model accurately simulated soybean root development considering soil physical limitation. The results show that the root length density (Fig. 12) can be altered in the soil profile due to rainfall deficit increasing the soil physical limitation to root growth. Mechanical impedance caused the larger stress in both weather conditions, wet and dry seasons. Stress due to matric potential was increased in a drought season favouring increment in total stress (Fig. 13). Root growth modelling with soil physical limitation is fundamental to improve the understanding about soybean response to drought stress, water use efficiency (Engels et al. 2017), evaporation and effective water uptake by roots (Manavalan et al. 2009).

Root length density and rooting depth were limited by drought stress (Fig. 12). Rooting depth was 25 cm deeper in wet season (75 cm depth) than in dry season (50 cm depth). This indicates that during drought season increased mechanical and hydric stress strongly reduced rooting depth. Roots grew deeper in conditions with higher water availability (wet season). This shows that root elongation responds directly to mechanical and hydric stress during the growth season. One of the major factors influencing soybean rooting depth is the taproot elongation rate (Manavalan et al. 2009) especially its response to soil physical conditions. In soils that impede root growth (e.g., because of a larger mechanical impedance), successive generations of roots tend to reuse paths of least mechanical resistance (Pierret et al. 2007), such as pre-existing structural features like cracks and biopores (Jin et al. 2013).Hydric limitation to water uptake and plant transpiration was increased in a drought season due smaller root system. Our model includes a physically based description of macroscopic root water uptake with an implicit compensation mechanism (de Jong van Lier et al. 2008). It is based on the matric flux potential only; further steps will need to include hydraulic resistances along the soil-plant-atmosphere

continuum (de Jong van Lier et al. 2013, Javaux et al. 2013). In the drought season, the combined effect of mechanical and hydric stress favours to reduce the root length density and to increase the number of days where hydric stress due to water uptake appeared. Rainfall deficit decreased the soil water content. This can increase the mechanical impedance exponentially (Moraes et al. 2012), and represents the main stress to root growth. That can favour a reduced plant transpiration due to physical barriers impeding root elongation (Tardieu 2013), decreasing the overall water flux from soil to rhizosphere (de Jong van Lier et al. 2013). In drought season smaller root systems took up only 50% of water compared to the wet season, and therefore acted as a major limitation to shoot development and grain yield (Saikumar et al. 2016). Water stress during early reproductive growth (flowering and pod set) reduces yield, usually as a result of fewer pods and seeds per unit area (Manavalan et al. 2009). For soybean the response of root growth to drought stress is controversial (Hirasawa et al. 1994; Franchini et al. 2017). In some experiment no reduction of root length density due to water stress during the vegetative growth was observed (Hirasawa et al. 1994). However, under different field conditions, soybean root length density was reduced strongly due drought during vegetative growth (Franchini et al. 2017). The consensus is that either way drought stress can be a major limitation to the production and yield stability of soybean (Manavalan et al. 2009). Therefore larger and deeper root systems are necessary to maintain water absorption (Lynch 2013; Tron et al. 2015) and plant transpiration for longer periods (Engels et al. 2017), with interaction of hydraulic conductivity in the soil and in the plant (Tardieu et al. 2017). As a consequence, optimum root systems for water uptake at a given time are not always those associated with the best yields (Tardieu et al. 2017).One substantial issue that remains is how to best simulate root growth in structured soils, where cracks and biopores offer low-resistance channels for root growth. The field experiment was performed on the Rhodic Eutrudox soil in a no-tillage system where many cracks and biopores were visible (Silva et al. 2014). By modifying the stress reduction function for penetration resistance (Eq. 16), it was possible to obtain qualitatively similar simulations of root growth (Fig. 15) comparable with field trench-wall root distribution maps. However, the importance of the exact relation between root elongation rate and penetration resistance, and how it might appropriately be modified to account for root penetrable pore-space, requires considerable further investigation potentially with more detailed simulation approaches such as explicit consideration of macropore geometry (e.g. see Landl et al. (2017)).

Eco-hydrological and root architecture models are important paths to increase the understanding of plant-environment interactions and plant physiological processes (Tron et al. 2015). Models of root functional architecture could also prove useful for crop improvement as they can be used to derive robust biophysical indexes characteristic of some crop–environmental combinations, such as improved root sink terms for water uptake modelling (Pierret et al. 2007). This work has considered the simulation of root growth and water uptake in relation to soil physical conditions and weather. The development of functional-structural models of root systems is a new way to account for root aging, in correlation with variation in physiological properties and to study the influence of age on the uptake at the plant scale (Vetterlein and Doussan 2016). Soil physical conditions affect shoot growth indirectly, by reducing the size and extent of a root system and so restricting the uptake of water and nutrients, if these are not abundant (Bengough 1997). They also may affect shoot growth directly via root-shoot signalling mechanisms (e.g. Masle and Passioura (1987)). A further step would be to consider how grain yield could be modelled from plant transpiration, although this adds a further tier of assumptions and complication to the approach.

The main novelty of this model is the combination of mechanical and hydric stresses and their application in a 3-D model of root growth. The response of root elongation to hydric and mechanical stresses has already been known, however their combined effect has never been applied in a model that considers individual stresses for each root (tap root, lateral and secondary root) over a whole cropping season. Also, variation of soil penetration resistance, water content and soil aeration (matric potential) has never been integrated into a root growth model. Thus we created a simple way to consider water flux in the soil-plant-atmosphere system, as well as the resulting variations in a stress reduction function (mechanical and hydric) for root elongation for each root and soil layer.

This is a model that describes the theoretical and applied framework that scientists could use to link weather and soil physical conditions to plant growth. Application of this model was exemplified for one field site in Brazil, considering two years with contrasting weather

conditions. However, this is only an example of model application; the model can be calibrated and used for different pedoclimatic conditions around the world.

One conceptual advance, that may be of immediate practical application is the use of diagrams such as in Fig. 4c and Fig. 4d to qualitatively explain the way that soil physical properties, weather and management system interact to restrict root growth. In addition, examples of Fig. 10 and Fig 13 can help to understand which physical stresses contribute more to reduction of root elongation, i.e. mechanical or hydric stresses. This type of diagram (Fig. 1,4) may be of help in teaching or explaining the interaction between plant physiological responses, soil properties and weather to both scientists and land managers.

Conclusions

This model represents a relatively simple approach to modelling root growth under different soil and weather conditions. The proposed framework with mechanical and hydric stresses implemented into the RootBox model offers a way to explore the interaction between soil physical properties, weather and root growth. In particular, it helps to explain the interaction between plant physiological responses and individual soil physical stresses. This root growth model separates the total stress reduction functions into two effects, one the penetration resistance (mechanical stress) and the other one the matric potential (aeration and water stress). The relative contribution of the stress reduction factor values favour understanding which physical stress contribute more for to reducing the root growth. It may be applied to most root elongation models, and offers the potential to evaluate likely factors limiting root growth in different soils and tillage regimes.

References

Addiscott TM, Whitmore AP (1987) Computer simulation of changes in soil mineral nitrogen and crop nitrogen during autumn, winter and spring. J Agric Sci 109:141 . doi: 10.1017/S0021859600081089

Allen RG, Pereira LS, Raes D, Smith M (1998) Crop evapotranspiration: Guidelines for computing crop requirements. Irrig Drain Pap No 56, FAO 300

Allen RG, Pereira LS, Smith M, et al (2005) Dual Crop Coef cient Method for Estimating Evaporation from Soil and Application Extensions. Irrig Drain 131:2–13 . doi: 10.1061/(ASCE)0733-9437(2005)131

Bengough AG (2006) Root responses to soil physical conditions; growth dynamics from field to cell. J Exp Bot 57:437–447 . doi: 10.1093/jxb/erj003

Bengough AG (2012) Root elongation is restricted by axial but not by radial pressures: So what happens in field soil? Plant Soil 360:15–18 . doi: 10.1007/s11104-012-1428-8

Bengough AG (1997) Modelling Rooting Depth and Soil Strength in a Drying Soil Profile. J Theor Biol 186:327–338 . doi: 10.1006/jtbi.1996.0367

Bengough AG, McKenzie BM, Hallett PD, Valentine TA (2011) Root elongation, water stress, and mechanical impedance: A review of limiting stresses and beneficial root tip traits. J Exp Bot 62:59–68 . doi: 10.1093/jxb/erq350

Bengough AG, Mullins CE (1991) Penetrometer resistance, root penetration resistance and root elongation rate in two sandy loam soils. Plant Soil 131:59–66 . doi: 10.1007/BF00010420

Benjamin JG, Nielsen DC (2006) Water deficit effects on root distribution of soybean, field pea and chickpea. F Crop Res 97:248–253 . doi: 10.1016/j.fcr.2005.10.005

Bodner G, Leitner D, Nakhforoosh A, et al (2013) A statistical approach to root system classification. Front Plant Sci 4:1–16 . doi: 10.3389/fpls.2013.00292

Bonfante A, Basile A, Acutis M, et al (2010) SWAP, CropSyst and MACRO comparison in two contrasting soils cropped with maize in Northern Italy. Agric Water Manag 97:1051–1062 . doi: 10.1016/j.agwat.2010.02.010

Busscher WJ (1990) Adjustment of flat-tipped penetrometer resistance data to a common water content. Trans ASAE 33:0519–0524 . doi: 10.13031/2013.31360

Casaroli D, de Jong van Lier Q, Dourado Neto D (2010) Validation of a root water uptake model to estimate transpiration constraints. Agric Water Manag 97:1382–1388 . doi: 10.1016/j.agwat.2010.04.004

931 Celia MA, Bouloutas ET (1990) A general Mass-Conservative Numerical solutuion for
932 Unsaturated flow equation. Water Resour Res 26:1483–1496
933 Clausnitzer V, Hopmans JW (1994) Simultaneous modeling of transient three-dimensional root
934 growth and soil water flow. Plant Soil 164:299–314 . doi: 10.1007/BF00010082
935 de Jong van Lier Q, van Dam JC, Durigon A, et al (2013) Modeling Water Potentials and Flows
936 in the Soil–Plant System Comparing Hydraulic Resistances and Transpiration Reduction
937 Functions. Vadose Zo J 12:1–20 . doi: 10.2136/vzj2013.02.0039
938 de Jong van Lier Q, van Dam JC, Metselaar K, et al (2008) Macroscopic Root Water Uptake
939 Distribution Using a Matric Flux Potential Approach. Vadose Zo J 7:1065 . doi:
940 10.2136/vzj2007.0083
941 Diggle AJ (1988b) Rootmap: a root growth model. Math Comput Simul 30:175–180 . doi:
942 10.1016/0378-4754(88)90121-8
943 Diggle AJ (1988a) ROOTMAP—a model in three-dimensional coordinates of the growth and
944 structure of fibrous root systems. Plant Soil 105:169–178 . doi: 10.1007/BF02376780
945 Dresbøll DB, Thorup-Kristensen K, McKenzie BM, et al (2013) Timelapse scanning reveals
946 spatial variation in tomato (Solanum lycopersicum L.) root elongation rates during partial
947 waterlogging. Plant Soil 369:467–477 . doi: 10.1007/s11104-013-1592-5
948 Dunbabin VM, Postma JA, Schnepf A, et al (2013) Modelling root-soil interactions using three-
949 dimensional models of root growth, architecture and function. Plant Soil 372:93–124 . doi:
950 10.1007/s11104-013-1769-y
951 Dupuy L, Gregory PJ, Bengough AG (2010) Root growth models: Towards a new generation of
952 continuous approaches. J Exp Bot 61:2131–2143 . doi: 10.1093/jxb/erp389
953 Engels C, Rodrigues F, Ferreira A, et al (2017) Drought Effects on Soybean Cultivation - A
954 Review. Annu Res Rev Biol 16:1–13 . doi: 10.9734/ARRB/2017/35232
955 Feddes RA, Kowalik PJ, Zaradny H (1978) Simulation of field water use and crop yield. Pudoc,
956 Wageningen, Netherlands
957 Foy CD (1992) Soil Chemical Factors Limiting Plant Root Growth. In: Hatfield J. L, Stewart BA
958 (eds) Advances in Soil Science: Limitations to Plant Root Growth, volume 19. Springer
959 New York, New York, NY, pp 97–131
960 Franchini JC, Balbinot Junior AA, Debiasi H, et al (2017) Root growth of soybean cultivars
961 under different water availability conditions. Semin Ciências Agrárias 38:715–724 . doi:
962 10.5433/1679-0359.2017v38n2p715
963 Greenwood DJ, Neeteson JJ, Draycott A (1985) Response of potatoes to N fertilizer: Dynamic
964 model. Plant Soil 85:185–203 . doi: 10.1007/BF02139623
965 Gregory PJ (2006) Plant Roots: Growth, Activity and Interaction with Soils. Blackwell Publishing
966 Ltd, Oxford, UK
967 Hartmann A, Šimůnek J (2016) Hydrus: Root Growth module, Version 1. Department of
968 Environmental Sciences, University of California Riverside, Riverside, California, USA
969 Hartmann A, Šimůnek J, Aidoo MK, et al (2017) Implementation and Application of a Root
970 Growth Module in HYDRUS. Vadose Zo J 0:0 . doi: 10.2136/vzj2017.02.0040
971 Hirasawa T, Tanaka K, Miyamoto D, et al (1994) Effects of Pre-Flowering Soil Moisture Deficits
972 on Dry Matter Production and Ecophysiological Characteristics in Soybean Plants under
973 Drought Conditions during Grain Filling. Japanese J Crop Sci 63:721–730 . doi:
974 10.1626/jcs.63.721
975 Iijima M, Kato J (2007) Combined Soil Physical Stress of Soil Drying, Anaerobiosis and
976 Mechanical Impedance to Seedling Root Growth of Four Crop Species. Plant Prod Sci
977 10:451–459 . doi: 10.1626/pps.10.451
978 Javaux M, Couvreur V, Vanderborght J, Vereecken H (2013) Root Water Uptake: From Three-
979 Dimensional Biophysical Processes to Macroscopic Modeling Approaches. Vadose Zo
980 Jounal 12:1–14 . doi: 10.2136/vzj2013.02.0042
981 Javaux M, Schröder T, Vanderborght J, Vereecken H (2008) Use of a Three-Dimensional
982 Detailed Modeling Approach for Predicting Root Water Uptake. Vadose Zo Jounal 7:1079–
983 1088 . doi: 10.2136/vzj2007.0115
984 Jin K, Shen J, Ashton RW, et al (2013) How do roots elongate in a structured soil? J Exp Bot
985 64:4761–4777 . doi: 10.1093/jxb/ert286
986 Jones CA, Bland WL, Ritchie JT, Williams JR (1991) Simulation of Root Growth. In: Hanks J,
987 Ritchie JT (eds) Modeling plant and soil systems, 31st edn. Agron. Monogr, ASA, CSSA,
988 SSSA, Madison, WI., pp 91–123
989 Kalogiros DI, Adu MO, White PJ, et al (2016) Analysis of root growth from a phenotyping data
990 set using a density-based model. J Exp Bot 67:1045–1058 . doi: 10.1093/jxb/erv573

991 Kroes JG, Van Dam JC, Groenendijk P, et al (2008) SWAP version 3.2. Theory description and
992 user manual. Alterra, Wageningen, Netherlands
993 Landl M, Huber K, Schnepf A, et al (2017) A new model for root growth in soil with macropores.
994 Plant Soil 415:99–116 . doi: 10.1007/s11104-016-3144-2
995 Leitner D, Klepsch S, Bodner G, Schnepf A (2010a) A dynamic root system growth model
996 based on L-Systems. Plant Soil 332:177–192 . doi: 10.1007/s11104-010-0284-7
997 Leitner D, Klepsch S, Knieß A, Schnepf A (2010b) The algorithmic beauty of plant roots – an L-
998 System model for dynamic root growth simulation. Math Comput Model Dyn Syst 16:575–
999 587 . doi: 10.1080/13873954.2010.491360
1000 Leitner D, Meunier F, Bodner G, et al (2014) Impact of contrasted maize root traits at flowering
1001 on water stress tolerance – A simulation study. F Crop Res 165:125–137 . doi:
1002 10.1016/j.fcr.2014.05.009
1003 Licht MA, Al-Kaisi M (2005) Strip-tillage effect on seedbed soil temperature and other soil
1004 physical properties. Soil Tillage Res 80:233–249 . doi: 10.1016/j.still.2004.03.017
1005 Lipiec J, Horn R, Pietrusiewicz J, Siczek A (2012) Effects of soil compaction on root elongation
1006 and anatomy of different cereal plant species. Soil Tillage Res 121:74–81 . doi:
1007 10.1016/j.still.2012.01.013
1008 Lynch JP (2013) Steep, cheap and deep: an ideotype to optimize water and N acquisition by
1009 maize root systems. Ann Bot 112:347–357 . doi: 10.1093/aob/mcs293
1010 Lynch JP, Nielsen KL, Davis RD, Jablokow AG (1997) SimRoot: Modelling and visualization of
1011 root systems. Plant Soil 188:139–151 . doi: 10.1023/A:1004276724310
1012 Manavalan LP, Guttikonda SK, Phan Tran L-S, Nguyen HT (2009) Physiological and Molecular
1013 Approaches to Improve Drought Resistance in Soybean. Plant Cell Physiol 50:1260–1276
1014 . doi: 10.1093/pcp/pcp082
1015 Masle J, Passioura J (1987) The Effect of Soil Strength on the Growth of Young Wheat Plants.
1016 Aust J Plant Physiol 14:643 . doi: 10.1071/PP9870643
1017 Miransari M (2016a) Soybean Tillage Stress. In: Miransari M (ed) Environmental Stresses in
1018 Soybean Production, 1st Ed. Elsevier, Amsterdam, pp 41–60
1019 Miransari M (2016b) Soybean Production and Compaction Stress. In: Miransari M (ed)
1020 Environmental Stresses in Soybean Production, 1st Ed. Elsevier, Amsterdam, pp 251–271
1021 Moraes MT de, Debiasi H, Carlesso R, et al (2017) Age-hardening phenomena in an oxisol from
1022 the subtropical region of Brazil. Soil Tillage Res 170:27–37 . doi:
1023 10.1016/j.still.2017.03.002
1024 Moraes MT de, Debiasi H, Carlesso R, et al (2016) Soil physical quality on tillage and cropping
1025 systems after two decades in the subtropical region of Brazil. Soil Tillage Res 155:351–
1026 362 . doi: 10.1016/j.still.2015.07.015
1027 Moraes MT de, Debiasi H, Franchini JC, Silva VR da (2012) Correction of resistance to
1028 penetration by pedofunctions and a reference soil water content. Rev Bras Ciência do
1029 Solo 36:1704–1713 . doi: 10.1590/S0100-06832012000600004
1030 Moraes MT de, Debiasi H, Franchini JC, Silva VR da (2013) Soil penetration resistance in a
1031 rhodic eutrudox affected by machinery traffic and soil water content. Eng Agrícola 33:748–
1032 757 . doi: 10.1590/S0100-69162013000400014
1033 Mualem Y (1976) A new model for predicting the hydraulic conductivity of unsaturated porous
1034 media. Water Resour Res 12:513–522 . doi: 10.1029/WR012i003p00513
1035 Ortigara C, Moraes MT de, Debiasi H, et al (2015) Modeling of soil load-bearing capacity as a
1036 function of soil mechanical resistance to penetration. Rev Bras Ciência do Solo 39:1036–
1037 1047 . doi: 10.1590/01000683rbcs20140732
1038 Pagès L, Bécel C, Boukcim H, et al (2014) Calibration and evaluation of ArchiSimple, a simple
1039 model of root system architecture. Ecol Modell 290:76–84 . doi:
1040 10.1016/j.ecolmodel.2013.11.014
1041 Pagès L, Jordan MO, Picard D (1989) A simulation model of the three-dimensional architecture
1042 of the maize root system. Plant Soil 119:147–154 . doi: 10.1007/BF02370279
1043 Pagès L, Vercambre G, Drouet J-L, et al (2004) Root Typ: a generic model to depict and
1044 analyse the root system architecture. Plant Soil 258:103–119 . doi:
1045 10.1023/B:PLSO.0000016540.47134.03
1046 Pereira LS, Allen RG, Smith M, Raes D (2015) Crop evapotranspiration estimation with FAO56:
1047 Past and future. Agric Water Manag 147:4–20 . doi: 10.1016/j.agwat.2014.07.031
1048 Pierret A, Doussan C, Capowiez Y, et al (2007) Root Functional Architecture: A Framework for
1049 Modeling the Interplay between Roots and Soil. Vadose Zo J 6:269–281 . doi:
1050 10.2136/vzj2006.0067

Postma JA, Kuppe C, Owen MR, et al (2017) OpenSimRoot: widening the scope and application of root architectural models. New Phytol 215:1274–1286 . doi: 10.1111/nph.14641
Prusinkiewicz P, Lindenmayer A (1990) The Algorithmic beauty of plants. Springer-Verlag, New York
Ritchie JT (1972) Model for predicting evaporation from a row crop with incomplete cover. Water Resour Res 8:1204–1213 . doi: 10.1029/WR008i005p01204
Rosa RD, Paredes P, Rodrigues GC, et al (2012) Implementing the dual crop coefficient approach in interactive software. 1. Background and computational strategy. Agric Water Manag 103:8–24 . doi: 10.1016/j.agwat.2011.10.013
Saglio PH, Rancillac M, Bruzan F, Pradet A (1984) Critical Oxygen Pressure for Growth and Respiration of Excised and Intact Roots. PLANT Physiol 76:151–154 . doi: 10.1104/pp.76.1.151
Saikumar S, Varma CMK, Saiharini A, et al (2016) Grain yield responses to varied level of moisture stress at reproductive stage in an interspecific population derived from Swarna /O . glaberrima introgression line. NJAS - Wageningen J Life Sci 78:111–122 . doi: 10.1016/j.njas.2016.05.005
Schmidt S, Gregory PJ, Grinev D V, Bengough AG (2013) Root elongation rate is correlated with the length of the bare root apex of maize and lupin roots despite contrasting responses of root growth to compact and dry soils. Plant Soil 372:609–618 . doi: 10.1007/s11104-013-1766-1
Schnepf A, Leitner D, Klepsch S (2012) Modeling Phosphorus Uptake by a Growing and Exuding Root System. Vadose Zo J 11: . doi: 10.2136/vzj2012.0001
Schnepf A, Leitner D, Landl M, et al (2017) CRootBox: A structural-functional 1 modelling framework for root systems 2. Biorxiv 3:139980 . doi: 10.1101/139980
Schnepf A, Leitner D, Schweiger PF, et al (2016) L-System model for the growth of arbuscular mycorrhizal fungi, both within and outside of their host roots. J R Soc Interface 13:1–11 . doi: 10.1098/rsif.2016.0129
Silva AP da, Babujia LC, Franchini JC, et al (2014) Soil structure and its influence on microbial biomass in different soil and crop management systems. Soil Tillage Res 142:42–53 . doi: 10.1016/j.still.2014.04.006
Silva AP da, Kay BD, Perfect E (1994) Characterization of the Least Limiting Water Range of Soils. Soil Sci Soc Am J 58:1775 . doi: 10.2136/sssaj1994.03615995005800060028x
Šimůnek J, Hopmans JW (2009) Modeling compensated root water and nutrient uptake. Ecol Modell 220:505–521 . doi: 10.1016/j.ecolmodel.2008.11.004
Tardieu F (2013) Plant response to environmental conditions: assessing potential production, water demand, and negative effects of water deficit. Front Physiol 4:1–11 . doi: 10.3389/fphys.2013.00017
Tardieu F, Draye X, Javaux M (2017) Root Water Uptake and Ideotypes of the Root System: Whole-Plant Controls Matter. Vadose Zo J 16:0 . doi: 10.2136/vzj2017.05.0107
Taylor HM, Ratliff LF (1969) Root elongation rates of cotton and peanuts as a function of soil strength and water content. Soil Sci 108:113–119
Taylor HM, Roberson GM, Parker JJ (1966) Soil strength-root penetration relations for medium- to coarse-textured soil materials. Soil Sci 102:18–22 . doi: 10.1097/00010694-196607000-00002
Tron S, Bodner G, Laio F, et al (2015) Can diversity in root architecture explain plant water use efficiency? A modeling study. Ecol Modell 312:200–210 . doi: 10.1016/j.ecolmodel.2015.05.028
Valentine TA, Hallett PD, Binnie K, et al (2012) Soil strength and macropore volume limit root elongation rates in many UK agricultural soils. Ann Bot 110:259–270 . doi: 10.1093/aob/mcs118
van Dam JC, Feddes RA (2000) Numerical simulation of infiltration, evaporation and shallow groundwater levels with the Richards equation. J Hydrol 233:72–85 . doi: 10.1016/S0022-1694(00)00227-4
van Genuchten MT (1980) A Closed-form Equation for Predicting the Hydraulic Conductivity of Unsaturated Soils. Soil Sci Soc Am J 44:892–898 . doi: 10.2136/sssaj1980.03615995004400050002x
Vereecken H, Schnepf A, Hopmans JW, et al (2016) Modeling Soil Processes: Review, Key Challenges, and New Perspectives. Vadose Zo J 15:1–57 . doi: 10.2136/vzj2015.09.0131
Vetterlein D, Doussan C (2016) Root age distribution: how does it matter in plant processes? A

1111 focus on water uptake. Plant Soil 407:145–160 . doi: 10.1007/s11104-016-2849-6
1112 Willmott CJ, Robeson SM, Matsuura K (2012) A refined index of model performance. Int J
1113 Climatol 32:2088–2094 . doi: 10.1002/joc.2419
1114 Wu L, McGechan MB, McRoberts N, et al (2007) SPACSYS: Integration of a 3D root
1115 architecture component to carbon, nitrogen and water cycling—Model description. Ecol
1116 Modell 200:343–359 . doi: 10.1016/j.ecolmodel.2006.08.010
1117 Wu Y, Cosgrove DJ (2000) Adaptation of roots to low water potentials by changes in cell wall
1118 extensibility and cell wall proteins. J Exp Bot 51:1543–1553 . doi:
1119 10.1093/jexbot/51.350.1543
1120

Table 1 Van Genuchten's parameter of a Rhodic Eutrudox under no-tillage system.

Depth	θs	θr	A	n	Ks	Bulk density
cm	$cm^3\ cm^{-3}$	$cm^3\ cm^{-3}$	cm^{-1}	--	$cm\ day^{-1}$	$Mg\ m^{-3}$
0-10	0.555	0.198	0.0892	1.1848	39.36	1.21
10-20	0.537	0.200	0.0822	1.1503	39.36	1.26
20-30	0.539	0.200	0.0756	1.1407	54.15	1.26
30-40	0.539	0.200	0.0756	1.1407	54.15	1.16
40-50	0.539	0.200	0.0756	1.1407	54.15	1.10
50-60	0.539	0.200	0.0756	1.1407	54.15	1.08
60-80	0.539	0.200	0.0756	1.1407	54.15	1.06
80-100	0.539	0.200	0.0756	1.1407	54.15	1.05

*θr, θs, α, and n are van Genuchten's parameters; Ks: hydraulic conductivity saturated;

Table 2 Root architectural parameters of soybean (*Glycine max*).

Symbol	Parameter name	units	Values [mean, s.d.]
Tap root			
r_e	Initial tip elongation rate	$cm\ day^{-1}$	[5.5, 0]
a	Root radius	cm	[0.2, 0]
l_a	Length of apical zone	cm	[2.0, 0]
l_b	Length basal zone	cm	[1.0, 0]
l_n	Internodal distance	cm	[0.65, 0]
n_b	Maximum number of branches	-	[300, 0]
σ	Expected change of root tip heading	$rad\ cm^{-1}$	0.4
type	Type of tropism	-	1
N	Strength of tropism	-	1.5
dx	Spatial resolution along root axis	cm	0.25
First-order laterals			
r_e	Initial tip elongation rate	$cm\ day^{-1}$	[1.5, 0]
a	Root radius	cm	[0.05, 0]
Θ	Insertion angle	rad	[1.2217, 0]
l_a	Length of apical zone	cm	[3, 0]
l_b	Length basal zone	cm	[3, 0]
l_n	Internodal distance	cm	[0.7, 0]
n_b	Maximum number of branches	-	[60, 0]
σ	Expected change of root tip heading	$rad\ cm^{-1}$	0.3
type	Type of tropism	-	1
N	Strength of tropism	-	0.1
dx	Spatial resolution along root axis	cm	0.25
Second-order laterals			
r_e	Initial tip elongation rate	$cm\ day^{-1}$	[1, 0]
a	Root radius	cm	[0.03, 0]
Θ	Insertion angle	rad	[1.22173, 0]
k	Maximal root length	cm	[2, 0]
σ	Expected change of root tip heading	$rad\ cm^{-1}$	0.4
type	Type of tropism	-	1
N	Strength of tropism	-	0
dx	Spatial resolution along root axis	cm	0.25
Basal roots			
r_e	Initial tip elongation rate	$cm\ day^{-1}$	[2, 0]
a	Root radius	cm	[0.06, 0]
Θ	Insertion angle	rad	[1.39626, 0]
l_a	Length of apical zone	cm	[15, 0]
l_b	Length basal zone	cm	[2, 0]
l_n	Internodal distance	cm	[2, 0]
n_b	Maximum number of branches	-	[40, 0]
σ	Expected change of root tip heading	$rad\ cm^{-1}$	0.1
type	Type of tropism	-	1
N	Strength of tropism	-	0.5
dx	Spatial resolution along root axis	Cm	0.25

s.d. is the standard deviation.

Table 3. Soybean growth stage date and crop and soil evaporation parameters for estimating evapotranspiration using the dual crop coefficient approach for a drought (2008/2009) and a wet season (2009/2010).

Parameters	Value	2008/2009	2009/2010
Crop transpiration*			
Kcb ini (20 days)	0-0.15	24/11 – 13/12	11/11 – 30/11
Kcb dev (35 days)	0.15-1.10	14/12 – 06/01	01/12 – 24/12
Kcb mid (40 days)	1.10	07/01 – 04/03	25/12 – 19/02
Kcb end (30 days)	1.10-0.30	05/03 – 29/03	20/02 – 16/03
Root sampling date		02/02/2009	20/01/2010
Soil evaporation			
REW (mm)		45	45
TEW (mm)		13.5	13.5
FC (m^3 m^{-3})		0.35	0.35
WP (m^3 m^{-3})		0.25	0.25
Ze (m)		0.10	0.10

*Basal crop coefficients (Kcb) were calculated during the crop growing season for initial (ini); crop development (Kcb dev); midseason (Kcb mid); and end season (Kcb end). TEW: total evaporable water; REW: readily evaporable water; FC: field capacity; WP: wilting point; Ze: thickness of the evaporation soil layer.

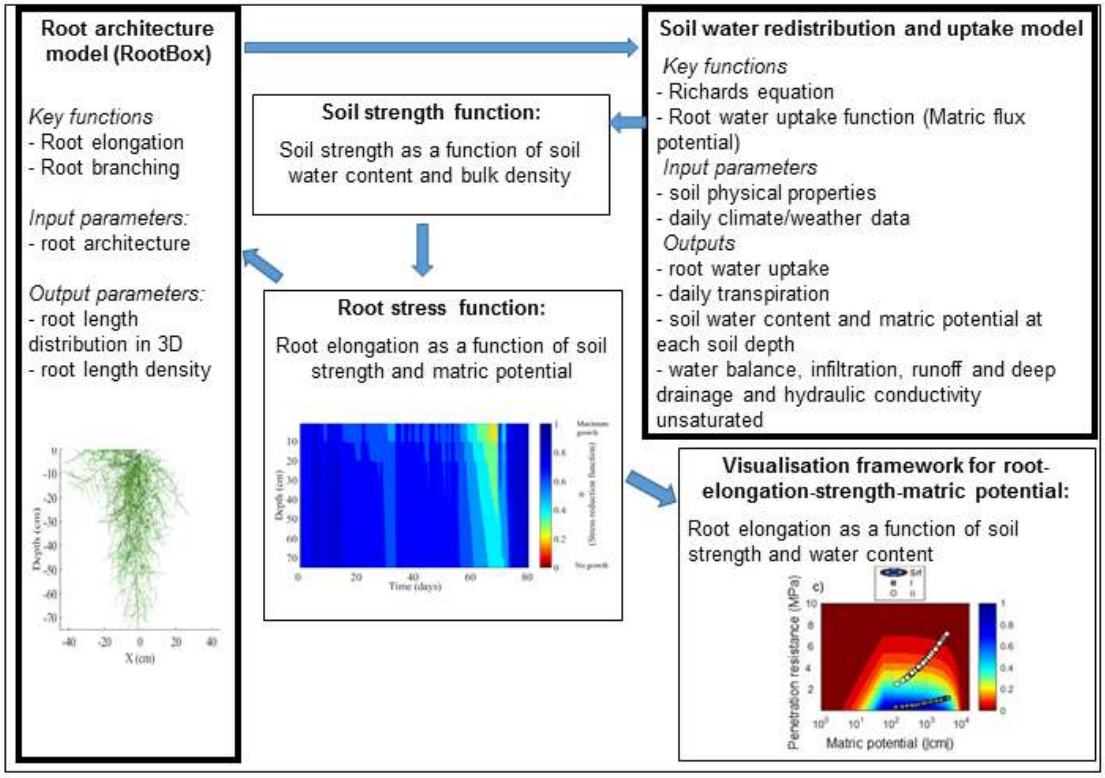

Fig. 1 Schematic representation of the model coupling in soil-root-plant-atmosphere relationship.

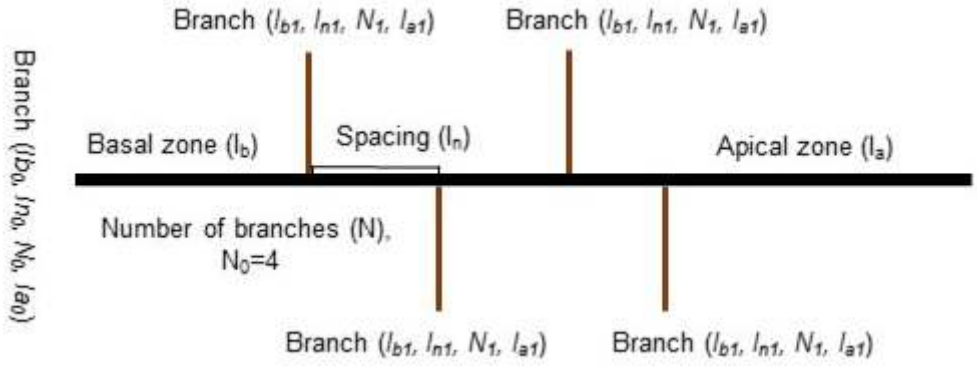

Fig. 2 An illustration of the self-similar characters of plant roots (Leitner et al. 2010b).

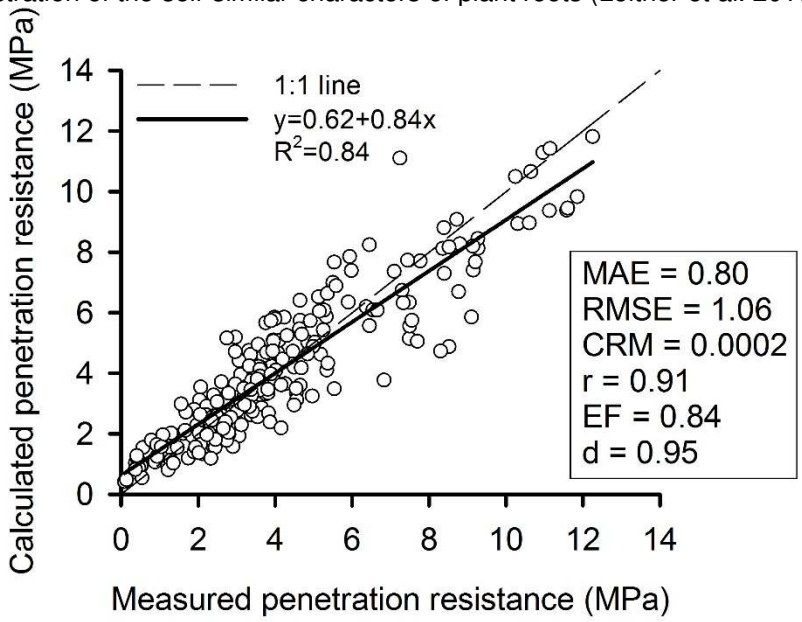

Fig. 3 Measured vs. calculated values of soil penetration resistance (Q_P) for a Rhodic Eutrudox, very clayed. Dashed line represents a one-to-one relationship. The Busscher's parameters were a=0.00587; b=8.0772; c=-4.65. The data set are from Ortigara et al. (2015). MAE: means absolute error; RMSE: root mean squared error; CRM: coefficient of residual mass; r: coefficient of correlation; EF: modelling efficiency; and d: index of agreement.

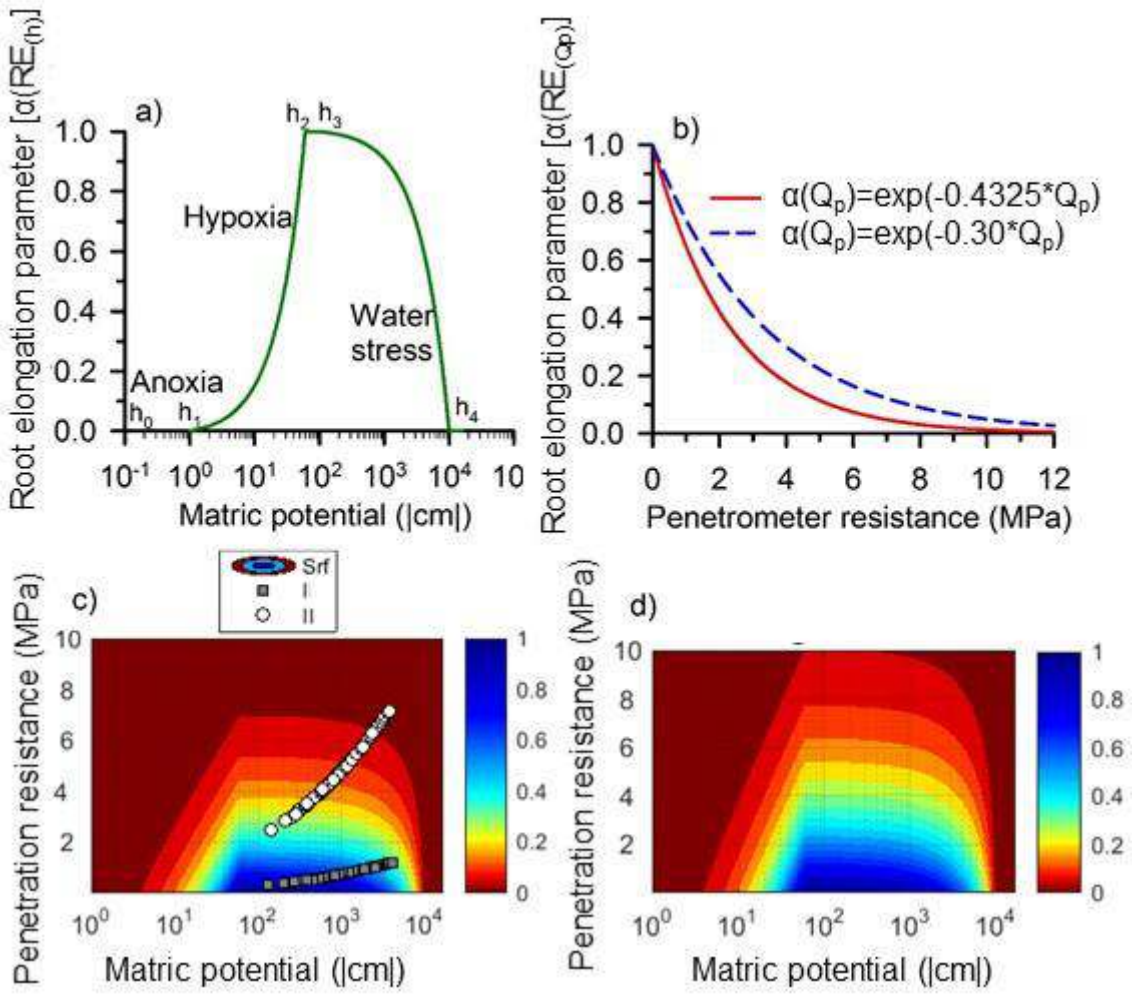

Fig. 4 Root elongation (RE) parameter as a function of matric potential (adapted from Feddes et al. (1978)) (a) and soil penetration resistance with presence (dashed blue line) or absence (red line adapted from Bengough (1997)) of continuous pores (b), and the total stress reduction function (srf) in a colour map for a soil without (c) or with (d) continuous pores. Root elongation parameter is expressed as an index from 1 (maximum root elongation) to 0 (no root growth). I: data set for a typical agricultural soil; II: data set for a compacted soil.

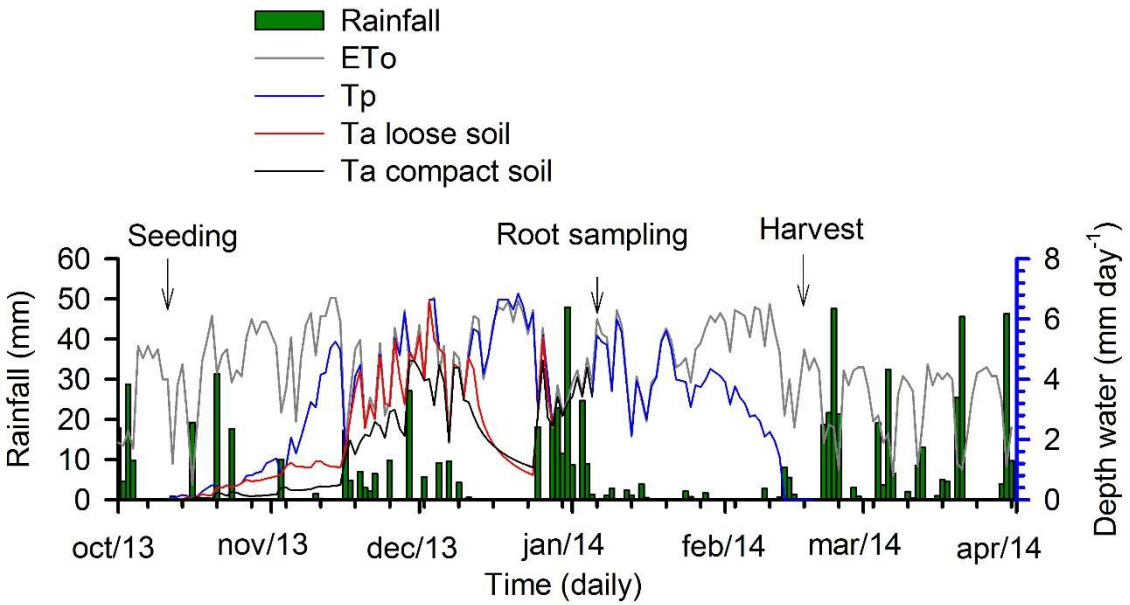

Fig. 5 Rainfall, reference evapotranspiration (ETo), potential transpiration (Tp) and actual transpiration (Ta) during soybean season growth in a loose soil and in a soil with a compact layer (data from Londrina, Brazil).

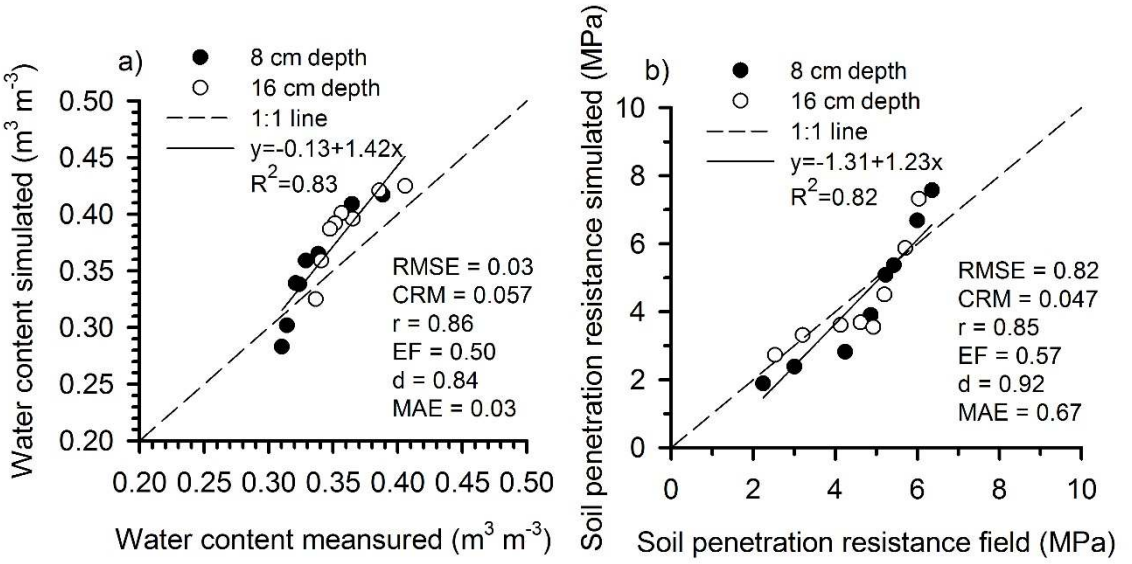

Fig. 6 Simulated and field measured values for water content (a) and soil penetration resistance (b) at 8 cm and 16 cm depths: points show average measured values under field conditions in Londrina/Brazil during a wet-dry cycle.

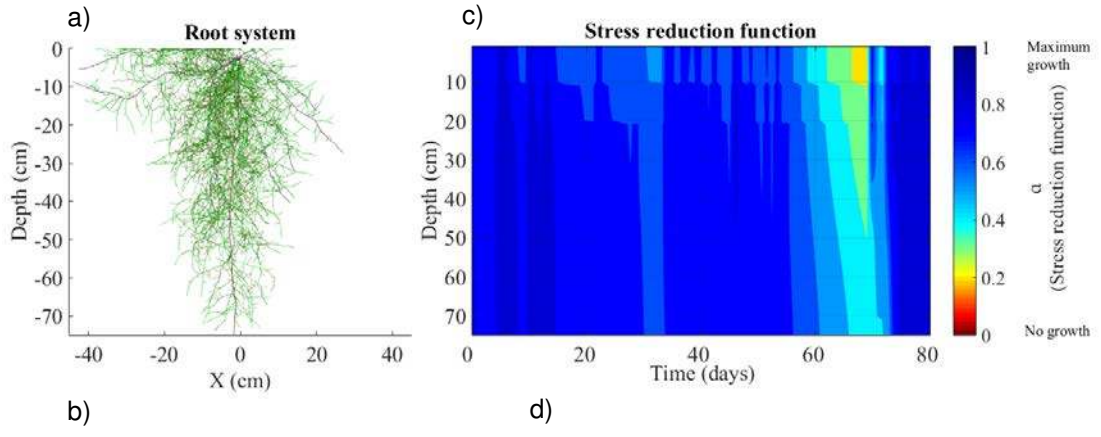

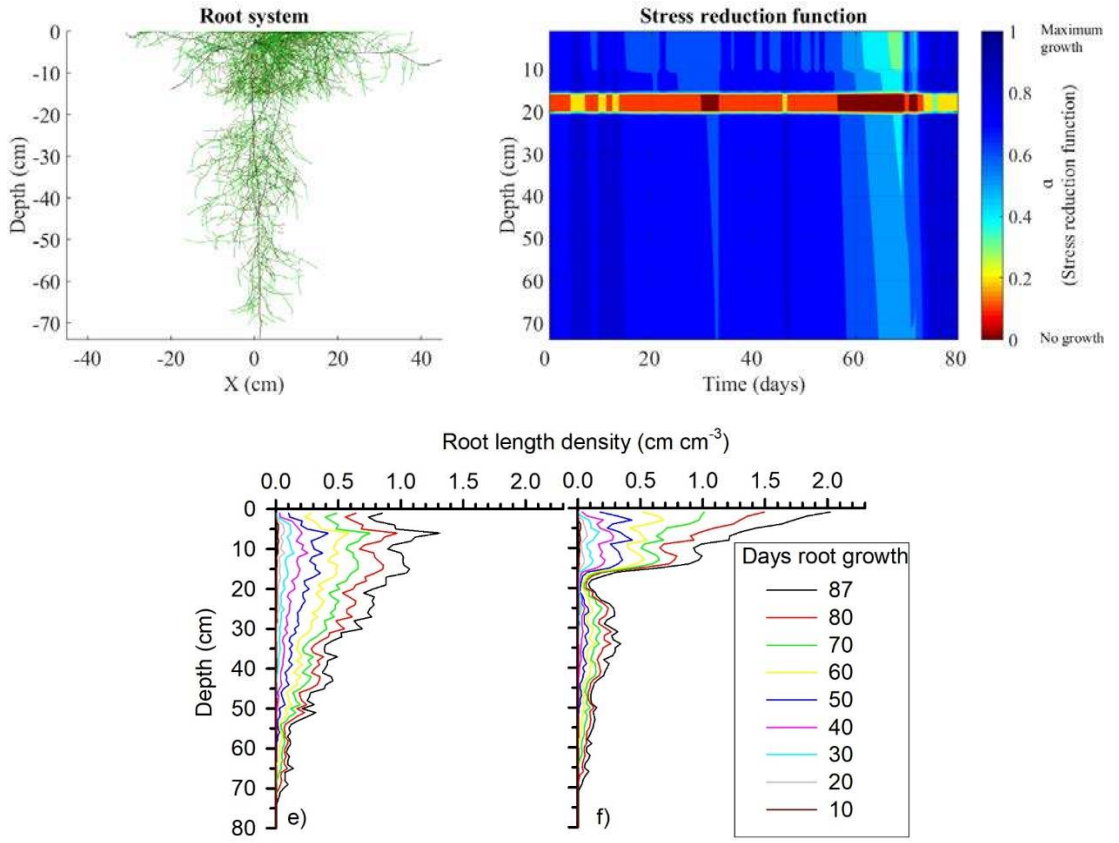

Fig. 7 Simulations of soybean root system distribution (a,b) and stress reduction funtion (c,d) and root length density over time (e,f) in soil without (a,c,e) or with (b,d,f) a compact layer from 16 to 20 cm. Timelapse video of root growth can seen at the supplementary material S1 (profile without soil compaction) and S1 (profile with a soil compacted layer).

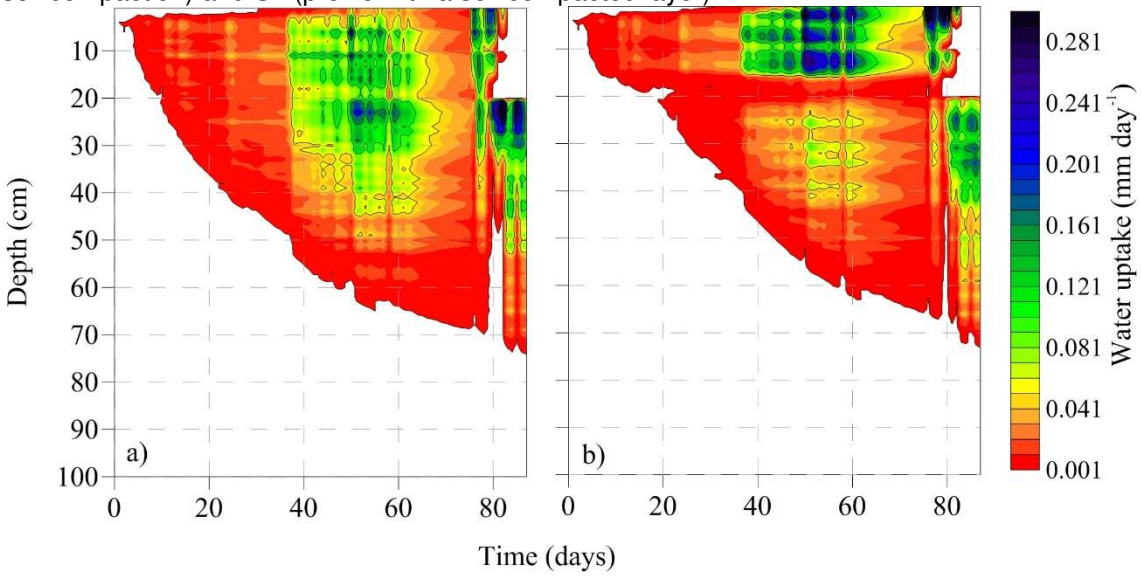

Fig. 8 Water uptake versus depth and time in (a) a soil with no compact layer, or (b) with a compact layer at 16-20 cm depth.

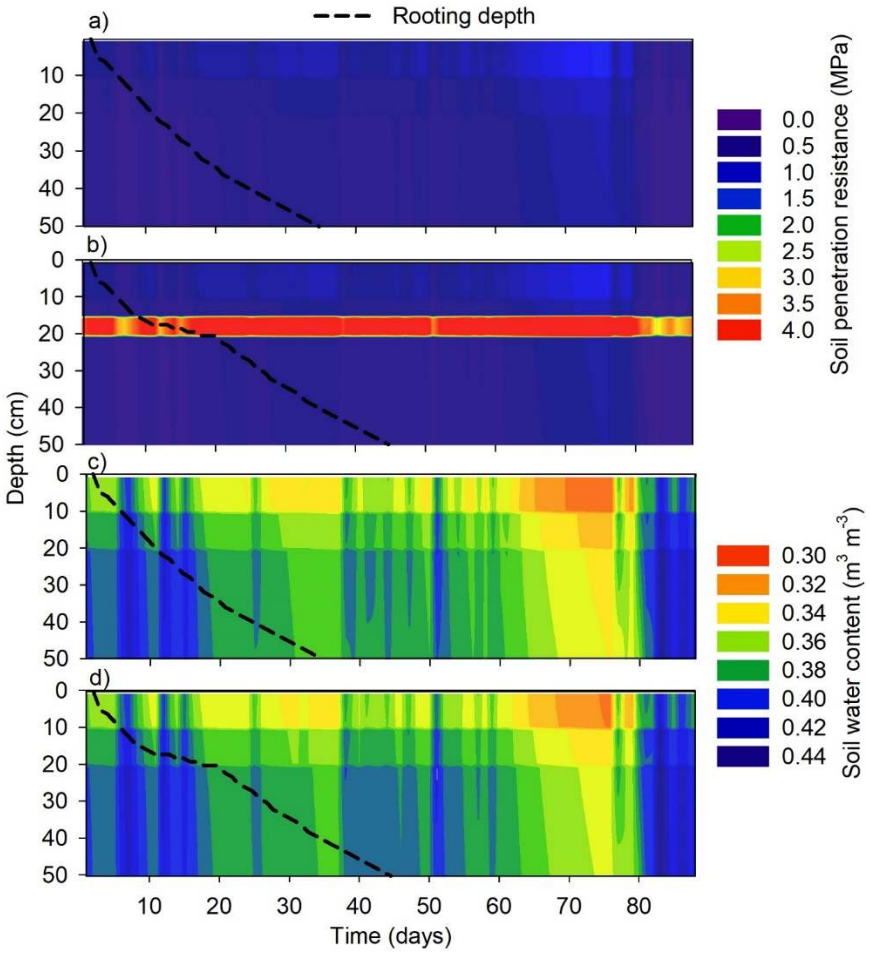

Fig. 9 Soil penetration resistance (a,b) and soil volumetric water content (c,d) in soil without compact layer (a,c), or in a soil with a compact layer (b,d).

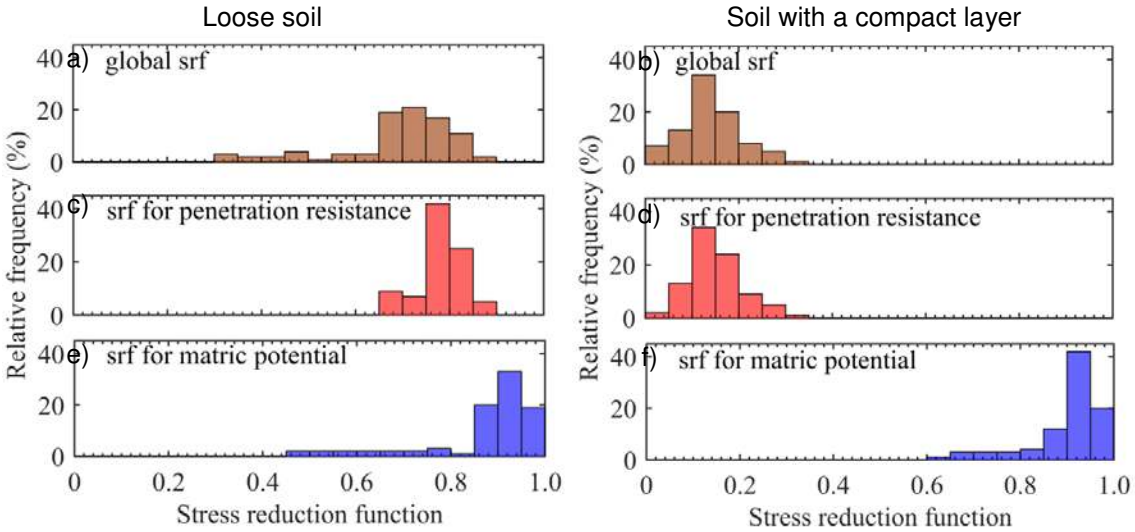

Fig. 10 Relative frequency of total stress reduction function (srf) (a,b) and effect from soil penetration resistance (c,d) or matric potential (e,f) and in the loose soil (a,c,e) or the soil with a compacted layer (b,d,f) from 16 to 20 cm depth.

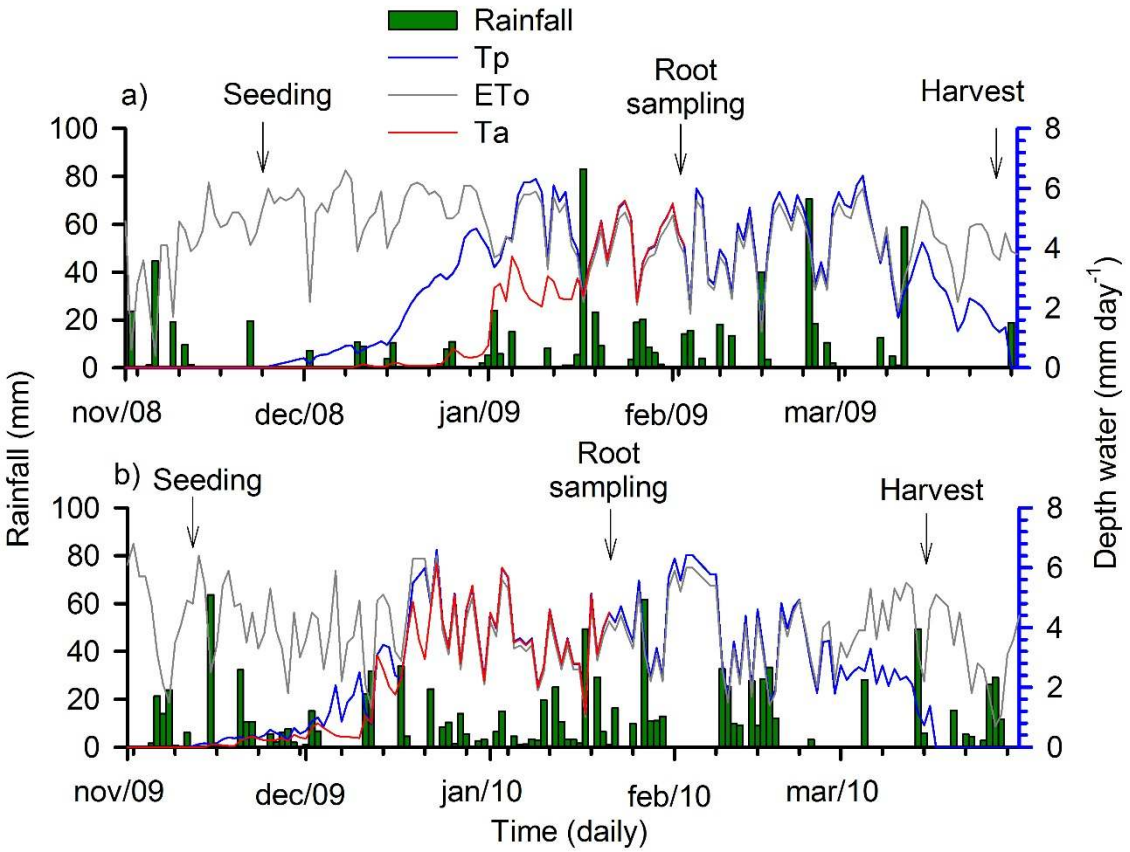

Fig. 11 Rainfall, reference evapotranspiration (Eto), potential (Tp) and actual transpiration (Ta) during soybean season growth in a drought – 2008/2009 (a) or a wetter season – 2009/2010 (b).

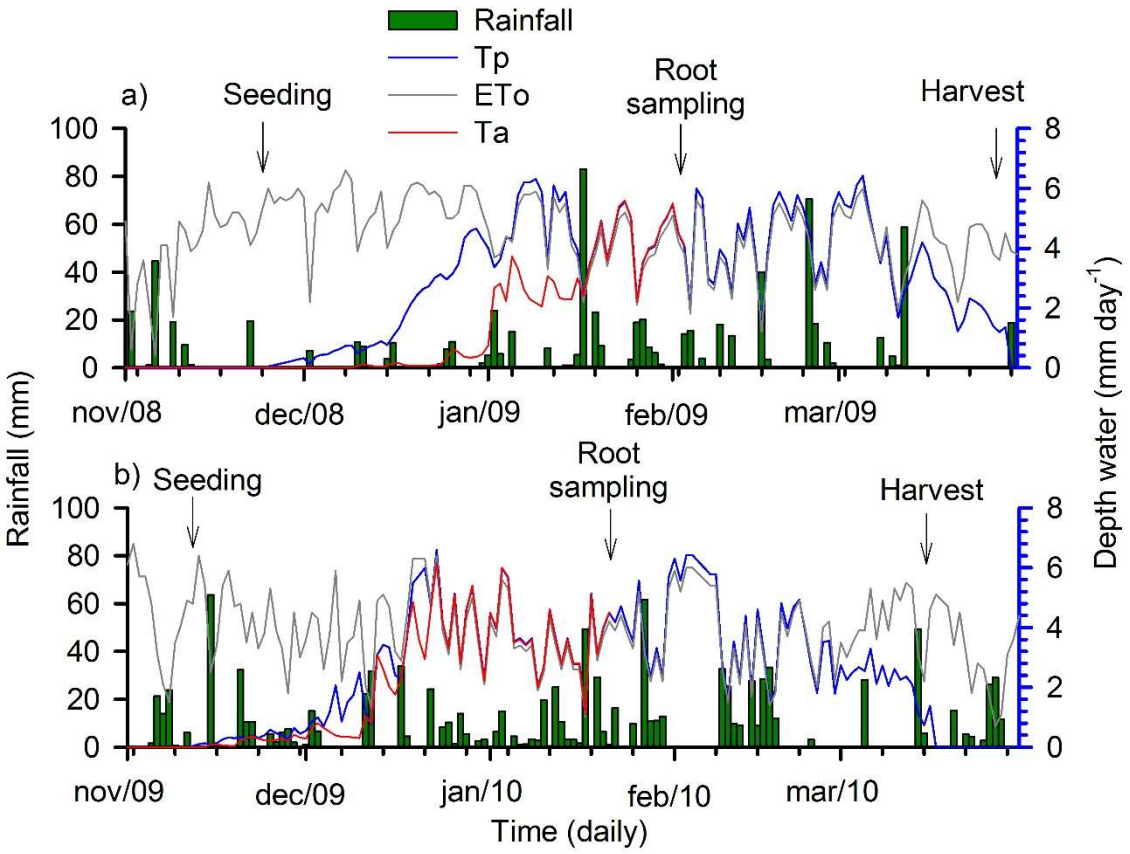

Fig. 11 Rainfall, reference evapotranspiration (Eto), potential (Tp) and actual transpiration (Ta) during soybean season growth in a drought – 2008/2009 (a) or a wetter season – 2009/2010 (b).

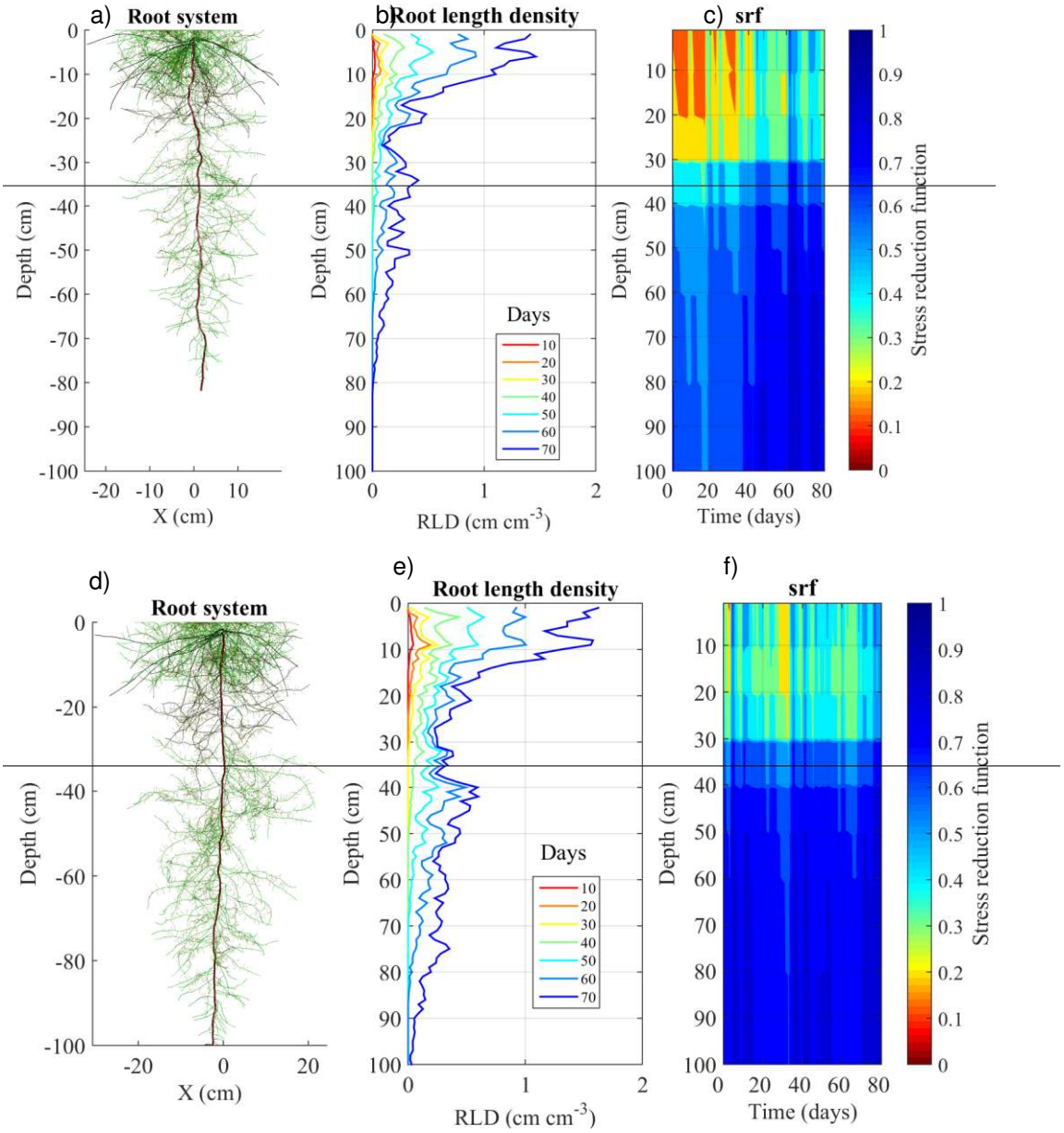

Fig. 12 Simulated soybean root system (a,d), root length density (RLD) (b,e) and stress reduction function (srf) (c,f) in the drier season (a,b,c) or wetter season (d,e,f) growth. Timelapse video of root growth can seen at the supplementary material S3 (drier season) and S4 (wetter season).

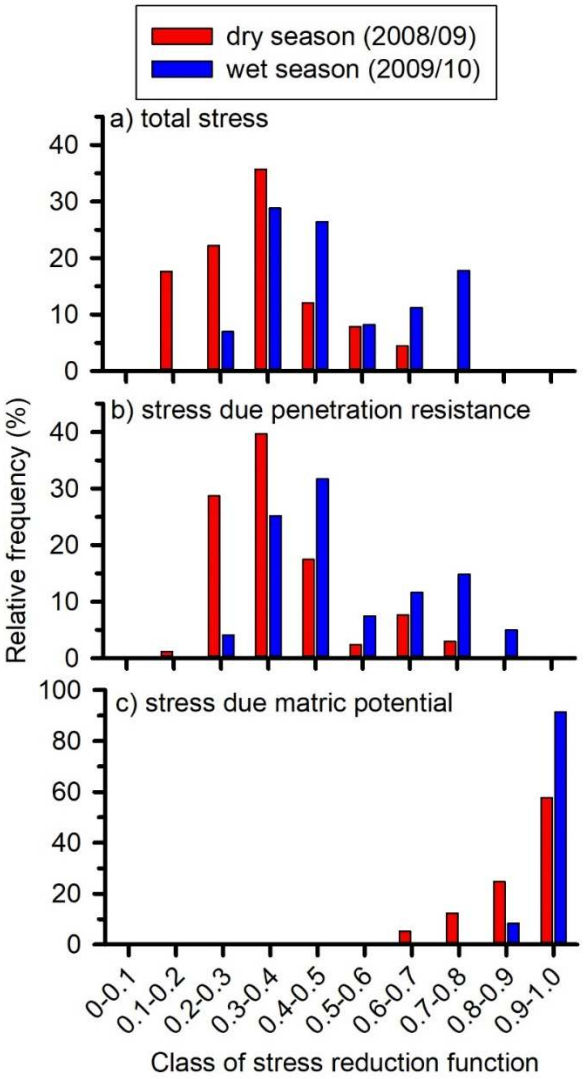

Fig. 13 Frequency of the total stress (a) or soil resistance to penetration (b) and matric potential (c) for root elongation in all rooting depth during the first 54 days of soybean growth in a Rhodic Eutrudox. Values close to zero correspond to the absence of growth, while values close to 1 mean maximum potential of root elongation.

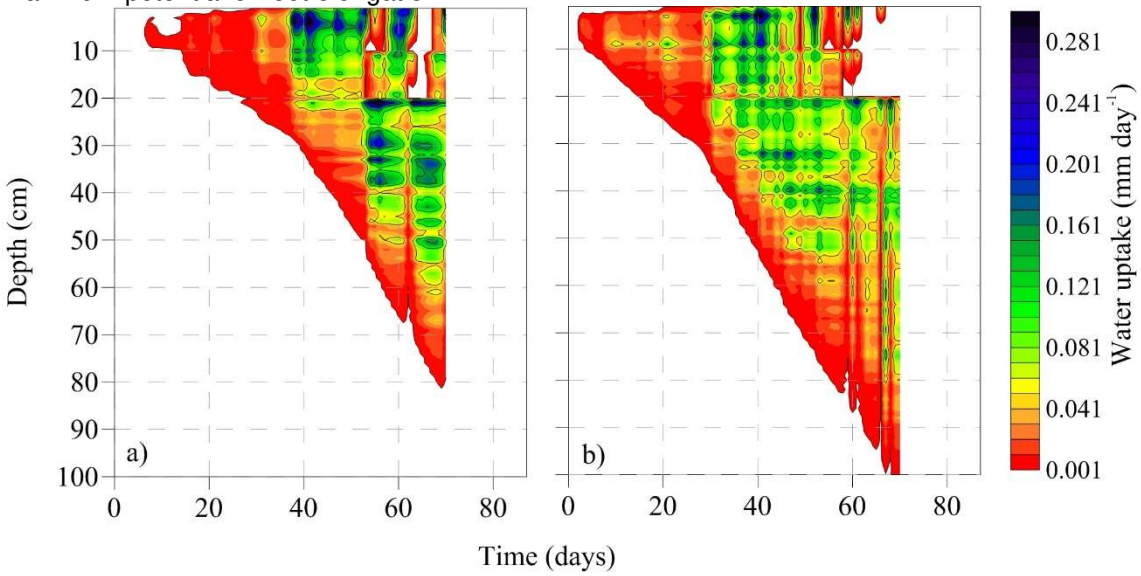

Fig. 14 Water uptake rate (mm per day) for a dry season (a) or a wet season (b) growth.

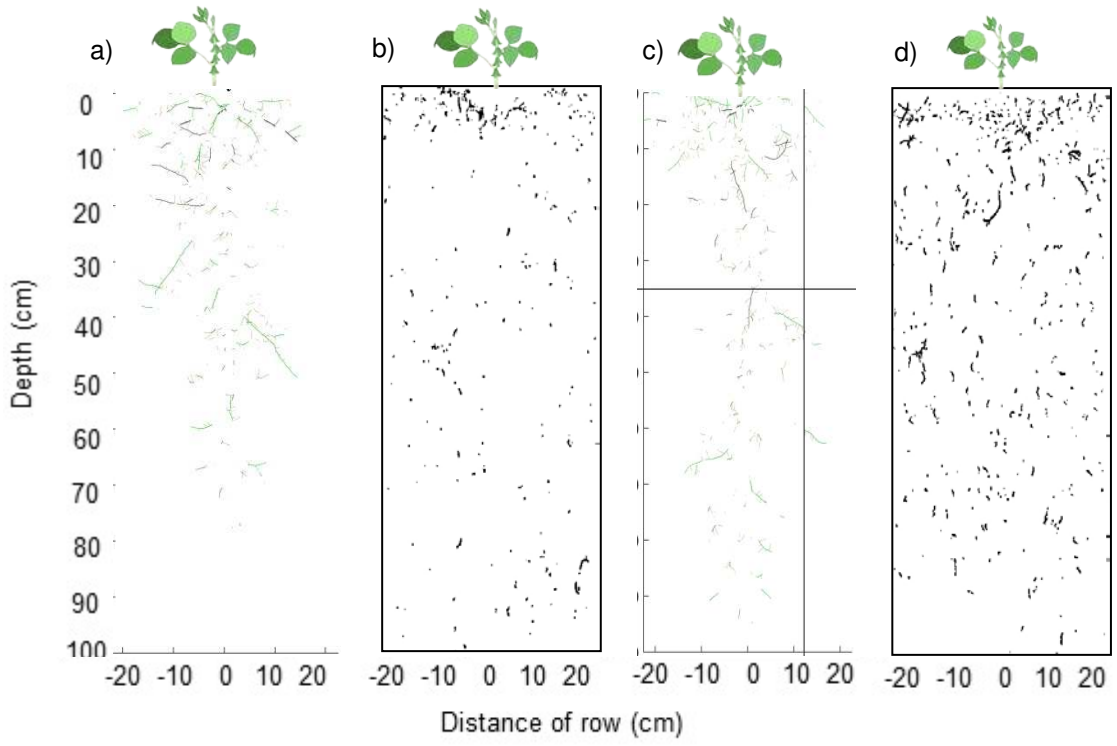

Fig. 15 Root system distribution simulated (a,c) and measured (b,d) for a dry (a,b) and wet season (c,d) at the soil profile (slice of 2 cm transversal to row).

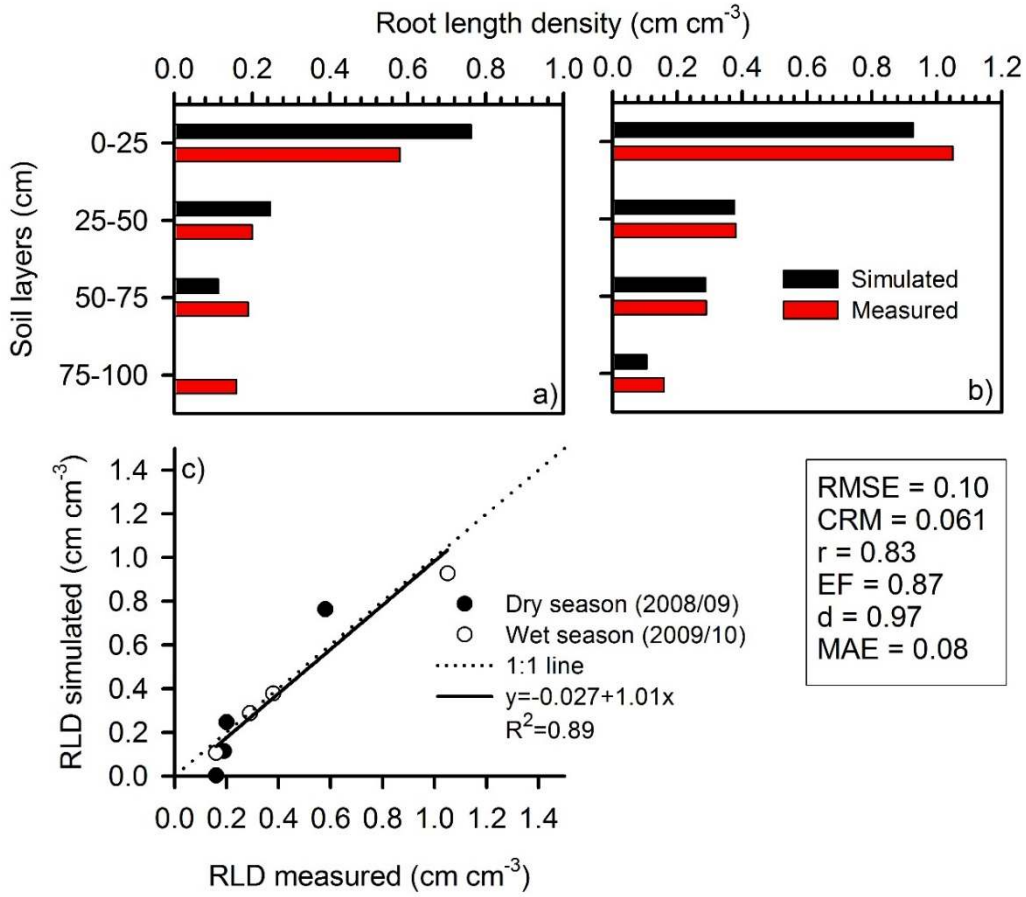

Fig. 16 Root length density measured on field and simulated for a dry season (a) and wet season (b) and relation 1 to 1 (c). *RMSE: root mean squared error; CRM: coefficient of residual mass; r:

coefficient of correlation; EF: modelling efficiency; d: index of agreement; MAE: means absolute error.